Author's personal copy

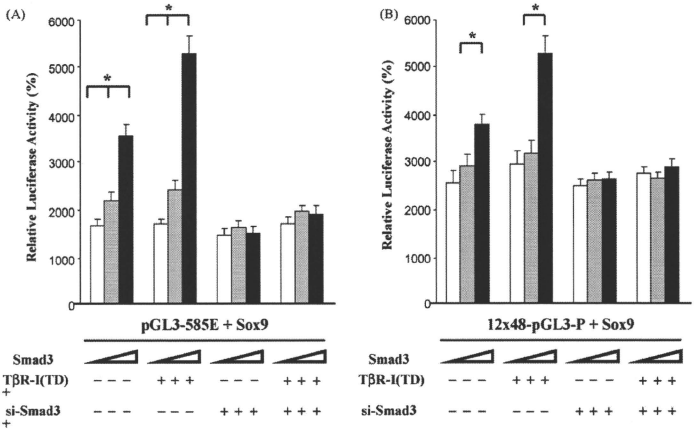

Fig. 2. Smad3 has an essential role for TGF-β-stimulated transactivation in the Sox9-regulated gene expression. (A) Smad3 enhanced the Sox9-dependent transcription in a dose-dependent manner. Smad3 and TβR-I(TD) synergistically increased the luciferase activity in pGL3-585E reporter systems. si-RNA against Smad3 (si-Smad3) totally inhibited the synergistic effects of Smad3 and TβR-I(TD). Note that si-Smad3 did not inhibit the Sox9-induced transactivation of reporter genes. (B) In 12 × 48 pGL3-P reporter systems, Smad3 and TβR-I(TD) cooperatively stimulated the relative luciferase activity up to 1.7-fold higher level in the presence of Sox9. A dose-dependent effect of Smad3 was observed. However, the increase of luciferase activity was suppressed by si-Smad3 in Smad3-transfected cells. Relative luciferase activities were calculated using the activity of pGL3-B (A) or pGL3-P (B) as a control (100%). Triangular boxes denote the transfection volume of Smad3 expression plasmid (0, 25, and 50 ng). *Statistical significances ($p < 0.05$) were observed between the indicated bars with the Mann–Whitney *U*-test. Error bars, S.D.

3.3. Recombinant Sox9 associates with p300 and binds to the Col2a1 enhancer in vitro

To examine the role of Sox9-associated transcriptional complex (Sox9, p300, and Smad3) on chromatin, we purified histones from HeLa cells, chromatin assembly-related molecules (NAP-1 and ACF complex), Sox9, p300, and Smad3 as described in Section 2. Purified NAP-1 and ACF sufficiently assembled chromatin under histone-containing conditions. Chromatin assembling abilities of these molecules were estimated by MNase digestion assays (Fig. 3A). Recombinant Sox9 purified from Sf9 cells associated with recombinant p300 in vitro (Fig. 3B). Recombinant Sox9 also bound with high affinity to the Col2a1 enhancer probe, which contains the Sox9-binding sequence, in EMSA (Fig. 3C).

3.4. TGF-β-stimulated Smad3 and p300 cooperatively activate the Sox9-dependent transcription on chromatin

For in vitro transcription analyses after chromatin assembly (Fig. 4A), we assessed the complex formation of Smad3 and Smad4. Smad3 purified from the nuclear fraction of TGF-β-treated Sf9 cells was a phosphorylated form of Smad3 (Fig. 4B). Smad4 was also detected in the same coimmunoprecipitated fraction using anti-FLAG M2 affinity gel (Fig. 4B). This result demonstrated that phosphorylated Smad3 was transferred into the nucleus with Smad4 by TGF-β treatment. In addition, purified Smad3/4 associated with recombinant Sox9 and p300 in vitro (Fig. 4C). Here we investigated the effect of phosphorylated Smad3 in the Sox9-dependent transcription on chromatin. In vitro transcription analyses on chromatinized templates revealed that the combination of Sox9, Smad3/4, and p300 were necessary for the activation of chromatin-mediated transcription (Fig. 4D). These findings suggest that the Sox9-dependent chondrogenesis might be strictly controlled by TGF-β signal Smad3 and chromatin remodeling factor p300.

4. Discussion

The present study indicates that TGF-β receptor-regulated Smad3 and p300 cooperatively activate the Sox9-dependent transcription on chromatin. The TGF-β signal plays an essential role to induce primary chondrogenesis (Pittenger et al., 1999; Heng et al., 2004). However, the differentiation of chondrocyte is regulated by the conflictive effects of TGF-β. TGF-β3 enhances the early chondrogenesis derived from mesenchymal stem cells (Fan et al., 2008). The short-term treatment with TGF-β3 has been reported to maintain a chondrogenic phenotype (Mehlhorn et al., 2006). On the other hand, TGF-β inhibits chondrocyte maturation at the late stage (Ballock et al., 1993; Ferguson et al., 2000). We previously described that TGF-β signal Smad3 promotes the early chondrogenesis through the activation of Sox9 (Furumatsu et al., 2005a). However, the cross-talk between TGF-β signal and Sox9 in the epigenetic regulation for initiating chondrogenesis is still unclear. Here, we further analyzed a crucial role of Smad3 in the Sox9-dependent chondrogenesis on chromatin. In this study, Smad3 enhanced the Sox9-mediated transcription in luciferase reporter assay systems (Fig. 1B and C). The increase of relative luciferase activity with Smad3 was higher in pGL3-585E, which contains a native set of Col2a1 promoter and enhancer, than in 12 × 48-pGL3-P systems. These findings might be caused by the binding affinity of Sox9 against each reporter plasmid. The activity of 12 × 48-pGL3-P containing high copies of Sox9-binding site might be already excited by the cotransfection of Sox9. A dose-dependent transactivation by Smad3 was observed in both systems,

Author's personal copy

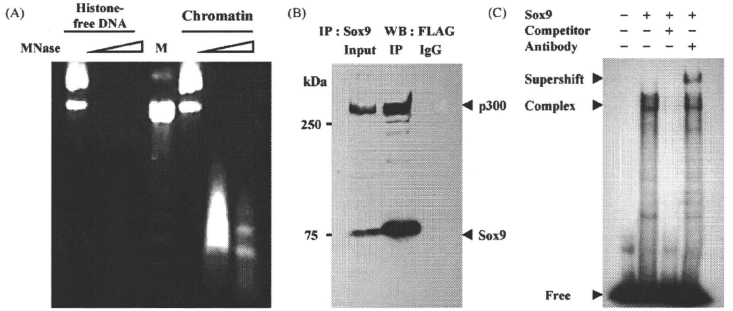

Fig. 3. MNase digestion analyses after chromatin assembly. Purified Sox9 form a complex with p300 or DNA probe containing the Sox9-binding site. (A) Closed circular 12 × 48-pGL3-P (300 ng) was used as a template. Chromatin assembling steps were performed as shown in Fig. 4A. Plasmid DNAs were completely digested by MNase (0.02 and 0.04 U/15 μl) in the absence of histones, NAP-1, and ACF (Histone-free DNA). Chromatinized plasmids were protected from complete digestion (Chromatin). Nucleosome-repeated pattern (approximately 165 bp) was observed in chromatin template after MNase treatment (0.04 U/15 μl). M, 123-bp ladder (Invitrogen). (B) Purified p300 was coimmunoprecipitated with recombinant Sox9 using anti-Sox9 antibody. Western blotting was performed with anti-FLAG M2 antibody. Sox9 (30 ng) was incubated with p300 (30 ng), and then the 10% of reaction was loaded as an input. Immunoprecipitation using rabbit IgG was performed as a control. Numbers indicate molecular weight (kDa). (C) Purified Sox9 associated with the Col2a1 enhancer probe in EMSA. The unlabeled competitor decreased the signal of Sox9–DNA complex. Supershifted band was observed in the presence of anti-Sox9 antibody.

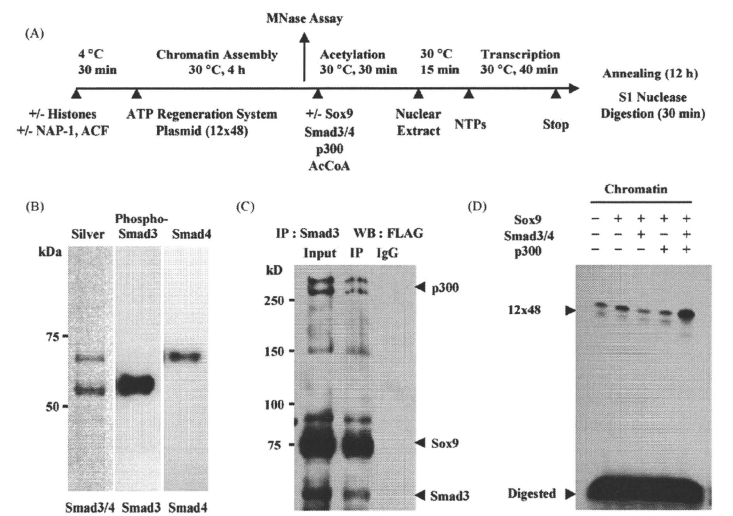

Fig. 4. Phosphorylated Smad3 and p300 cooperatively activate the Sox9-dependent transcription on chromatin. (A) The sequential steps for chromatin assembly and in vitro transcription are illustrated. MNase assays were performed after chromatin assembly (Fig. 3A). To estimate the amounts of RNAs transcribed from chromatinized plasmid, S1 nuclease assays were performed as described in Section 2. S1 nuclease digests a single-stranded part of RNA and excessive primers. Remaining double-stranded fragments (49-bp), which are annealed with ^{32}P end-labeled specific primers, represent transcriptional activities on chromatin. (B) Recombinant Smad3/4 were prepared using baculovirus expression systems. The details are described in Section 2. Smad3/4 complex were visualized with silver staining (left lane). Phosphorylated Smad3 were obtained after TGF-β treatments (middle lane). Smad4 was coimmunoprecipitated with FLAG-tagged Smad3 (right lane). (C) Protein–protein interactions among recombinant proteins. Purified Sox9 (50 ng), p300 (50 ng), and Smad3/4 (50/15 ng) were incubated, and then immunoprecipitated with anti-Smad2/3 antibodies. Sox9 and p300 were coimmunoprecipitated with Smad3 (IP). Western blotting analyses were performed with anti-FLAG M2 antibodies. (D) Sox9, Smad3/4, and p300 cooperatively enhanced the transcriptional activities of chromatinized 12 × 48-pGL3-P (12 × 48, upper bands). Chromatin-mediated transcription was not fully activated by the combined treatment with Sox9 and Smad3/4 (or p300). Note that the synergistic effect of triple combination with Sox9, Smad3/4, and p300 was observed (right lane). Digested denotes non-annealed probes, which were digested by S1 nuclease treatments (lower bands).

Author's personal copy

and was totally suppressed by the cotransfection of si-RNA against Smad3 itself (Fig. 2). We previously demonstrated that si-Smad3 completely decreased the Col2a1 expression in a mesenchymal stem cell-derived chondrogenic model (Furumatsu et al., 2005a). These results suggest that Smad3 is the major transducer of TGF-β signal in the Sox9-regulated early chondrogenesis.

The Sox9-dependent transcription is synergistically activated by p300 on chromatin (Furumatsu et al., 2005b). Transcriptional coactivator p300 has an important role for gene expression and cellular differentiation (Dilworth et al., 2004; Espinosa and Emerson, 2001; Kitagawa et al., 2003). The effect of p300 is exerted through several mechanisms. p300 acts as a protein scaffold and a bridging factor for forming transcriptional complexes. In addition, the intrinsic histone acetyltransferase activity of p300 has a potential to facilitate the transcriptional activity by modulating chromatin structure (Chan and La Thangue, 2001; Korzus et al., 1998; Utley et al., 1998). Several authors have reported that p300 plays a critical role for the activation of cAMP response element-binding protein-, MyoD-, p53-, or vitamin D receptor-dependent transcription on reconstituted chromatin (Asahara et al., 2001; Dilworth et al., 2004; Espinosa and Emerson, 2001; Kitagawa et al., 2003). In previous studies, we described that p300 and Smad3 enhanced the Sox9-dependent transcription by associating with Sox9 (Tsuda et al., 2003; Furumatsu et al., 2005a). However, the precise effect of the third associating factor, such as Smad3, on chromatin is still unclear. To analyze the additional effect of the third factor in a chromatin assembly model is considered to be hard. This study revealed the additional effect of phosphorylated Smad3 in the Sox9- and p300-mediated transcription using 12 × 48-pGL3-P-based chromatin assembly model (Fig. 4D). However, the synergistic effect of Smad3 was not observed in a different balance of Sox9-associating molecules (data not shown). In pGL3-585E systems, we could not detect a significant effect of Smad3 on chromatin-derived transcription, either (data not shown). These findings suggest that the balance of Sox9-associating factors and the accessibility to chromatinized promoter might be important for the epigenetic regulation of chondrogenesis. In addition, the discrepancy of Smad3-induced transactivation between reporter assays (Figs. 1 and 2) and chromatin-derived transcription (Fig. 4D) might be caused by the following reasons: (i) the chromatinized status of Sox9-reactive plasmid was different in each analysis, (ii) the influence of Sox9 and p300 was more critical on chromatin-assembled plasmid, and (iii) unknown factors in SW1353 nuclear extracts might have important roles in the Sox9-dependent transcription on chromatin. Several transcription partners such as Sox-5/6, PGC-1α, Barx2, and TRAP230 can modify the Sox9-dependent transcription during chondrogenesis (Ikeda et al., 2004; Kawakami et al., 2005; Lefebvre et al., 2001; Meech et al., 2005; Zhou et al., 2002). Further analyses to identify the other unknown partners of Sox9-based transcriptional complex will be required.

Animal models for a loss of Smad3 function have revealed the importance of Smad3 in physiological systems. Smad3 null mice show skeletal defects including osteoarthritis (Datto et al., 1999). Haploinsufficiency of Smad2 and Smad3 causes an embryonic lethality due to endodermal defects and exhibits craniofacial defects (Liu et al., 2004). We previously reported that Smad3 had an important role for primary chondrogenesis (Furumatsu et al., 2005a). In addition to the Smad3 pathway, TGF-β activates mitogen-activated protein kinase (MAPK) pathway during chondrogenic differentiation (Stanton et al., 2003). Several authors have shown that MAPK pathway modulates Col2a1 and Sox9 expression in chondrogenesis (Murakami et al., 2000; Nakamura et al., 1999; Tuli et al., 2003). These reports suggest that TGF-β-stimulated MAPK pathway would also be involved in chondrogenesis with modifying the Sox9-dependent transcription. Further studies to analyze the relationships between MAPK pathway and the Sox9-mediated transcription on chromatin are required.

In conclusion, the present study demonstrates that Smad3 enhances the Sox9-dependent transcription on chromatin. Our findings suggest the potential molecular mechanism how TGF-β signals induce early chondrogenesis via chromatin regulation.

Acknowledgements

We thank B. de Crombrugghe, T. Imamura, T. Ito, Y. Yamada, and TP. Yao for providing us with plasmids and baculovirus. We are also grateful to M. Lotz and our colleagues at the Department of Molecular and Experimental Medicine for their great support during this study.

This work was supported in part by grants from NIH (AR50631), JST SORST, Genome Network Project (MEXT), Grants-in Aid for Scientific Research (MEXT), Research on Child Health and Development, Research on Publicly, Essential Drugs and Medical Device (Japan Health Sciences Foundation) (H.A.), Japan Society for the Promotion of Science (grant-in-aid for scientific research 18890115 and 20791040), and Japanese Foundation for Research and Promotion of Endoscopy, and by a fellowship conferred from Uehara Memorial Foundation (T.F.).

Appendix A. Supplementary data

Supplementary data associated with this article can be found, in the online version, at doi:10.1016/j.biocel.2008.10.032.

References

Akiyama H, Chaboissier MC, Martin JF, Schedl A, de Crombrugghe B. The transcription factor Sox9 has essential roles in successive steps of the chondrocyte differentiation pathway and is required for expression of Sox5 and Sox6. Genes Dev 2002;16:2813–28.

Akiyama H, Lyons JP, Mori-Akiyama Y, Yang X, Zhang R, Zhang Z, et al. Interactions between Sox9 and β-catenin control chondrocyte differentiation. Genes Dev 2004;18:1072–87.

Asahara H, Santoso B, Guzman E, Du K, Cole PA, Davidson I, et al. Chromatin-dependent cooperativity between constitutive and inducible activation domains in CREB. Mol Cell Biol 2001;21:7892–900.

Asahara H, Tartare-Deckert S, Nakagawa T, Ikehara T, Hirose F, Hunter T, et al. Dual roles of p300 in chromatin assembly and transcriptional activation in cooperation with nucleosome assembly protein 1 in vitro. Mol Cell Biol 2002;22:2974–83.

Ballock RT, Heydemann A, Wakefield LM, Flanders KC, Roberts AB, Sporn MB. TGF-β 1 prevents hypertrophy of epiphyseal chondrocytes: regulation of gene expression for cartilage matrix proteins and metalloproteases. Dev Biol 1993;158:414–29.

Bell DM, Leung KK, Wheatley SC, Ng LJ, Zhou S, Ling KW, et al. SOX9 directly regulates the type-II collagen gene. Nat Genet 1997;16:174–8.

Chan HM, La Thangue NB. p300/CBP proteins: HATs for transcriptional bridges and scaffolds. J Cell Sci 2001;114:2363–73.

Datto MB, Frederick JP, Pan L, Borton AJ, Zhuang Y, Wang XF. Targeted disruption of Smad3 reveals an essential role in transforming growth factor beta-mediated signal transduction. Mol Cell Biol 1999;19:2495–504.

Dilworth FJ, Seaver KJ, Fishburn AL, Htet SL, Tapscott SJ. In vitro transcription system delineates the distinct roles of the coactivators pCAF and p300 during MyoD/E47-dependent transactivation. Proc Natl Acad Sci USA 2004;101:11593–8.

Espinosa JM, Emerson BM. Transcriptional regulation by p53 through intrinsic DNA/chromatin binding and site-directed cofactor recruitment. Mol Cell 2001;8:57–69.

Fan H, Zhang C, Li J, Bi L, Qin L, Wu H, et al. Gelatin microspheres containing TGF-β3 enhance the chondrogenesis of mesenchymal stem cells in modified pellet culture. Biomacromolecules 2008;9:927–34.

Felsenfeld G, Groudine M. Controlling the double helix. Nature 2003;421:448–53.

Ferguson CM, Schwarz EM, Reynolds PR, Puzas JE, Rosier RN, O'Keefe RJ. Smad2 and 3 mediate transforming growth factor-β1-induced inhibition of chondrocyte maturation. Endocrinology 2000;141:4728–35.

Furumatsu T, Tsuda M, Taniguchi N, Tajima Y, Asahara H. Smad3 induces chondrogenesis through the activation of SOX9 via CREB-binding protein/p300 recruitment. J Biol Chem 2005a;280:8350–843.

Furumatsu T, Tsuda M, Yoshida K, Taniguchi N, Ito T, Hashimoto M, et al. Sox9 and p300 cooperatively regulate chromatin-mediated transcription. J Biol Chem 2005b;280:35203–8.

Author's personal copy

Heldin CH, Miyazono K, ten Dijke P. TGF-β signalling from cell membrane to nucleus through SMAD proteins. Nature 1997;390:465–71.
Heng BC, Cao T, Lee EH. Directing stem cell differentiation into the chondrogenic lineage in vitro. Stem Cells 2004;22:1152–67.
Ikeda T, Kamekura S, Mabuchi A, Kou I, Seki S, Takato T, et al. The combination of SOX5, SOX6, and SOX9 (the SOX trio) provides signals sufficient for induction of permanent cartilage. Arthritis Rheum 2004;50:3561–73.
Ito T, Bulger M, Kobayashi R, Kadonaga JT. Drosophila NAP-1 is a core histone chaperone that functions in ATP-facilitated assembly of regularly spaced nucleosomal arrays. Mol Cell Biol 1996;16:3112–24.
Ito T, Levenstein ME, Fyodorov DV, Kutach AK, Kobayashi R, Kadonaga JT. ACF consists of two subunits, Acf1 and ISWI, that function cooperatively in the ATP-dependent catalysis of chromatin assembly. Genes Dev 1999;13:1529–39.
Ito T, Ikehara T, Nakagawa T, Kraus WL, Muramatsu M. p300-mediated acetylation facilitates the transfer of histone H2A–H2B dimers from nucleosomes to a histone chaperone. Genes Dev 2000;14:1899–907.
Jaenisch R, Bird A. Epigenetic regulation of gene expression: how the genome integrates intrinsic and environmental signals. Nat Genet 2003;33(Suppl):245–54.
Kawakami Y, Tsuda M, Takahashi S, Taniguchi N, Esteban CR, Zemmyo M, et al. Transcriptional coactivator PGC-1α regulates chondrogenesis via association with Sox9. Proc Natl Acad Sci USA 2005;102:2414–9.
Kitagawa H, Fujiki R, Yoshimura K, Mezaki Y, Uematsu Y, Matsui D, et al. The chromatin-remodeling complex WINAC targets a nuclear receptor to promoters and is impaired in Williams syndrome. Cell 2003;113:905–17.
Korzus E, Torchia J, Rose DW, Xu L, Kurokawa R, McInerney EM, et al. Transcription factor-specific requirements for coactivators and their acetyltransferase functions. Science 1998;279:703–7.
Lefebvre V, Behringer RR, de Crombrugghe B. L-Sox5, Sox6 and Sox9 control essential steps of the chondrocyte differentiation pathway. Osteoarthritis Cartilage 2001;9:S69–75.
Li E. Chromatin modification and epigenetic reprogramming in mammalian development. Nat Rev Genet 2002;3:662–73.
Liu Y, Festing M, Thompson JC, Hester M, Rankin S, El-Hodiri HM, et al. Smad2 and Smad3 coordinately regulate craniofacial and endodermal development. Dev Biol 2004;270:411–26.
Meech R, Edelman DB, Jones FS, Makarenkova HP. The homeobox transcription factor Barx2 regulates chondrogenesis during limb development. Development 2005;132:2135–46.
Mehlhorn AT, Niemeyer P, Kaiser S, Finkenzeller G, Stark GB, Südkamp NP, et al. Differential expression pattern of extracellular matrix molecules during chondrogenesis of mesenchymal stem cells from bone marrow and adipose tissue. Tissue Eng 2006;12:1393–403.
Murakami S, Kan M, McKeehan WL, de Crombrugghe B. Up-regulation of the chondrogenic Sox9 gene by fibroblast growth factors is mediated by the mitogen-activated protein kinase pathway. Proc Natl Acad Sci USA 2000;97:1113–8.
Nakagawa T, Bulger M, Muramatsu M, Ito T. Multistep chromatin assembly on supercoiled plasmid DNA by nucleosome assembly protein-1 and ATP-utilizing chromatin assembly and remodeling factor. J Biol Chem 2001;276:27384–91.
Nakamura K, Shirai T, Morishita S, Uchida S, Saeki-Miura K, Makishima F. p38 mitogen-activated protein kinase functionally contributes to chondrogenesis induced by growth/differentiation factor-5 in ATDC5 cells. Exp Cell Res 1999;250:351–63.
Ng LJ, Wheatley S, Muscat GE, Conway-Campbell J, Bowles J, Wright E, et al. SOX9 binds DNA, activates transcription, and coexpresses with type II collagen during chondrogenesis in the mouse. Dev Biol 1997;183:108–21.
Pittenger MF, Mackay AM, Beck SC, Jaiswal RK, Douglas R, Mosca JD, et al. Multilineage potential of adult human mesenchymal stem cells. Science 1999;284:143–7.
Shi Y, Massagué J. Mechanisms of TGF-β signaling from cell membrane to the nucleus. Cell 2003;113:685–700.
Stanton LA, Underhill TM, Beier F. MAP kinases in chondrocyte differentiation. Dev Biol 2003;263:165–75.
Stricker S, Fundele R, Vortkamp A, Mundlos S. Role of Runx genes in chondrocyte differentiation. Dev Biol 2002;245:95–108.
Tsuda M, Takahashi S, Takahashi Y, Asahara H. Transcriptional co-activators CREB-binding protein and p300 regulate chondrocyte-specific gene expression via association with Sox9. J Biol Chem 2003;278:27224–9.
Tuli R, Tuli S, Nandi S, Huang X, Manner PA, Hozack WJ, et al. Transforming growth factor-β-mediated chondrogenesis of human mesenchymal progenitor cells involves N-cadherin and mitogen-activated protein kinase and Wnt signaling cross-talk. J Biol Chem 2003;278:41227–36.
Utley RT, Ikeda K, Grant PA, Cote J, Steger DJ, Eberharter A, et al. Transcriptional activators direct histone acetyltransferase complexes to nucleosomes. Nature 1998;394:498–502.
Zhou R, Bonneaud N, Yuan CX, de Santa Barbara P, Boizet B, Schomber T, et al. SOX9 interacts with a component of the human thyroid hormone receptor-associated protein complex. Nucleic Acids Res 2002;30:3245–52.

Inflamm. res. 57 (2008) 4–10
1023-3830/07/010004-7
DOI 10.1007/s00011-007-7036-z

© Birkhäuser Verlag, Basel, 2008

Inflammation Research

Inhibition of histone deacetylase down-regulates the expression of hypoxia-induced vascular endothelial growth factor by rheumatoid synovial fibroblasts

H. Manabe[1,3], Y. Nasu[1], T. Komiyama[1], T. Furumatsu[1,2], A. Kitamura[1], S. Miyazawa[1], Y. Ninomiya[3], T. Ozaki[1], H. Asahara[2,4] and K. Nishida[1,5]

[1] Department of Orthopaedic Surgery, Science of Functional Recovery and Reconstruction, Okayama University, Okayama, Japan
[2] Department of Molecular and Experimental Medicine, The Scripps Research Institute, 10550 North Torrey Pines Road, La Jolla, CA 92037, USA
[3] Department of Molecular Biology and Biochemistry, Okayama University, Okayama, Japan
[4] National Research Institute for Child Health and Development, 2-10-1 Okura, Setagaya, Tokyo 157-8535, Japan
[5] Department of Human Morphology, Okayama University Graduate School of Medicine, Dentistry and Pharmaceutical Sciences, 2-5-1 Shikata-cho, Okayama City, Okayama 700-8558, Japan, Fax: ++81 86 223 9727, e-mail: knishida@md.okayama-u.ac.jp

Received 28 February 2007; returned for revision 19 March 2007; accepted by J. Di Battista 11 July 2007

Abstract. *Objective:* To investigate the effect of FK228 on the *in vitro* expression of hypoxia-inducible factor-1 alpha (HIF-1α) and vascular endothelial growth factor (VEGF) by rheumatoid arthritis synovial fibroblasts (RASFs), and on the *in vivo* expression of VEGF and angiogenesis in the synovial tissue of mice with collagen-antibody-induced arthritis (CAIA).
Methods: RASFs were stimulated with IL-1β and TNFα and then incubated under hypoxia (1 % O_2) with various concentrations of FK228. The effects of FK228 on the expression of HIF-1α and VEGF mRNA were examined by quantitative real-time PCR. Changes in HIF-1α protein expression and the secretion of VEGF protein into the culture medium were examined by Western blot analysis and ELISA, respectively. Immunohistochemical analysis was carried out to investigate the expression and distribution of VEGF in synovial tissues of CAIA mice.
Results: The cytokine-stimulated expression of HIF-1α and VEGF mRNA was inhibited by FK228 in a dose-dependent manner. FK228 also reduced the expression of HIF-1α and VEGF protein. Intravenous administration of FK228 (2.5 mg/kg) suppressed VEGF expression, and also blocked angiogenesis in the synovial tissue of CAIA.
Conclusion: FK228 may exhibit a therapeutic effect on RA by inhibition of angiogenesis through down-regulation of angiogenesis related factors, HIF-1α and VEGF.

Key words: Histone deacetylase (HDAC) – Rheumatoid arthritis – Vascular endothelial growth factor (VEGF) – Hypoxia-inducible factor-1 (HIF-1)

Correspondence to: K. Nishida

Introduction

Angiogenesis is an essential component in the formation and maintenance of inflammatory synovial tissues in rheumatoid arthritis (RA) [1] as it allows these tissues to cope with the increased demand for oxygen and nutrients [2]. Previous studies demonstrated that the inhibition of angiogenesis ameliorated synovial inflammation in animal models of arthritis [3], suggesting that blockade of angiogenesis offered a promising therapeutic strategy for RA. However, the patho-mechanisms that control the development of synovial angiogenesis in RA are not fully understood.

Several growth factors, including fibroblast growth factors (FGFs), vascular endothelial growth factor (VEGF), platelet-derived endothelial cell growth factor (PD-ECGF), as well as soluble forms of several adhesion molecules are able to stimulate angiogenesis directly by interacting with endothelial cell receptors [4]. VEGF is of particular importance in the process of angiogenesis as it promotes endothelial cell migration and increases vascular permeability [5]. It is known that RA synoviocytes secrete VEGF, and synovial fluids in RA patients contain abnormally high levels of VEGF [6, 7]. Accordingly, the VEGF receptors flt-1 and flk-1 are strongly expressed in endothelial cells of the RA synovium [4]. In clinical studies, administration of anti-TNFα antibody reduced serum levels of VEGF by up to 40 % in patients with RA; however, circulating VEGF levels remained significantly higher than in healthy individuals [2]. Therefore, anti-angiogenic agents, including antibodies to VEGF and VEGF receptor antagonists, are currently being tested for their therapeutic use in RA [8–12].

There are many angiogenic and angiostatic factors that regulate VEGF expression [5]. In all cell types studied to date, two transcription factors, hypoxia-inducible factor-1 (HIF-1) and HIF-2, which are induced to similar levels

under hypoxic conditions, were shown to stimulate the VEGF gene promoter. While the HIF-1α subunit is rapidly degraded under normoxic conditions, under hypoxic conditions, it is stabilized and translocates to the nucleus, where it transactivates a number of genes with hypoxia-responsive elements in their promoters [13]. The HIF-2α subunit is highly expressed by vascular endothelial cells and activates the transcription of endothelial-cell-specific receptor tyrosine kinase and the VEGF receptor flk-1. A previous study demonstrated significant cytoplasmic and nuclear overexpression of HIF-1α and HIF-2α in the synovial lining and stromal cells in RA and in osteoarthritis synovial tissue [14]. More recently, Makino et al. reported that CD3-positive T cells which had accumulated in inflammatory tissue expressed HIF-1α [15]. The authors postulated that hypoxia plays an important role in the survival of activated T cells via the HIF-1α-adrenomedullin cascade. These findings suggest that HIF-1α is closely involved in synovial pathology and can thus serve as a therapeutic target for RA.

It has been shown that histone modification through reversible acetylation is a crucial event in gene expression [16]. Histone acetylation is controlled by two enzymes, histone acetyltranferase (HAT) and histone deacetylase (HDAC) [17, 18]. Increasing evidence indicates that the antitumor activity of HDAC inhibitors is exerted through multiple mechanisms, such as apoptosis, cell cycle arrest, and differentiation, via the modulation of gene expression [19–24]. Recent reports demonstrated that specific HDAC inhibitors, including trichostatin A (TSA) and depsipeptide (FK228), inhibit angiogenesis by altering HIF-1 expression and VEGF signaling [25–27]. This finding raised the questions whether HDAC inhibitor prevents angiogenesis within the inflammatory joint by repressing hypoxia-induced HIF-1 and VEGF expression by rheumatoid arthritis synovial fibroblasts (RASFs). To answer that question, we investigated the *in vitro* effects of FK228, a specific HDAC inhibitor, on the expression of HIF-1α and VEGF by RASFs under hypoxic conditions. In addition, the *in vivo* effects of FK228 on the expression of VEGF and the number of blood vessels in synovial tissue were studied in mice with collagen-antibody-induced arthritis (CAIA). The results demonstrated a potential for beneficial role of HDAC inhibitors in blockage of angiogenesis *via* suppression of angiogenesis-related factors in RA synovial tissue.

Materials and methods

Reagents

Recombinant human IL-1β and TNFα were purchased from R&D Systems (Minneapolis, MN), stored at –80 °C, and diluted in culture medium immediately before use. Mouse monoclonal antibody against HIF-1α was purchased from Novus Biologicals, Inc. (Littleton, CO). Rabbit polyclonal antibody against VEGF (A-20) was purchased from Santa Cruz Biotechnology, Inc. (CA, USA). FK228 was provided by Fujisawa Pharmaceutical Co., Ltd. (Osaka, Japan). For the *in vitro* studies, FK228 was dissolved in DMSO and diluted with each of the experimental media before use. For the *in vivo* studies, FK228 was dissolved in and diluted with 10 % polyoxythylene (60)-hydrogenated castor oil in saline (HCO60 saline).

Isolation and culture of human RASFs

Following the written permission of the patients, fresh synovial tissues were obtained from five RA patients during total joint replacement surgery. The tissues were minced and then immediately digested with collagenase (Wako, Osaka, Japan) and DNAase (Sigma-Aldrich) at 37 °C, as previously described [28]. Tissue debris was removed with a cell strainer, and the remaining cells were washed twice with Dulbecco's modified Eagle's medium (DMEM, Sigma-Aldrich) supplemented with 10 % HEPES (Life Technologies, Tokyo, Japan), 100 IU penicillin/ml, and 100 mg streptomycin/ml (Life Technologies). The resultant single-cells were dispensed into the wells of a 24-well microtiter plate (Costar, Cambridge, MA) at a density of 2×10^6 cells/ml in 2 ml of DMEM supplemented with 10 % fetal bovine serum (FBS; Life Technologies, Rockville, MD), 100 IU penicillin/ml, and 100 mg streptomycin/ml. The plates were incubated at 37 °C in a humidified atmosphere containing 5 % CO_2. Synovial-tissue cell cultures were divided once weekly until the primary cultures had reached confluence. After the third passage, morphologically homogeneous fibroblast-like cells were obtained.

Hypoxic conditions

A sealed chamber (ASTEC APM-30D, Fukuoka, Japan) was used to culture cell preparations in a low-oxygen-tension environment of 1 % O_2, 5 % CO_2, and 94 % N_2.

Quantitative real-time PCR for the detection of HIF-1α and VEGF mRNA

Cells were seeded at a density of 1×10^6/well in 6-well culture dishes, stimulated with recombinant human IL-1β (1 ng/ml) and recombinant human TNFα (10 ng/ml) for 1 h, and then incubated with or without various concentrations of FK228 under 1 % O_2 for up to 24 h. The morphology of the cells was examined under polarized light microscopy, after which total RNA was isolated from cultured cells using Isogen reagent (Nippon Genhe, Toyama, Japan). The purified RNA was reverse-transcribed using Rever Tra Ace (Toyobo, Tokyo, Japan).

For real-time PCR, the primer sequences of HIF-1α and VEGF were as follows: for HIF-1α, 5 -ATC ATG CAG CTA CTA CAT CA-3 (forward) and 5 -CTT CAC AAT CAT AAC TGG TC-3 (reverse); for VEGF, 5 -TCT TCA AGC CAT CCT GTG T-3 (forward) and 5 -CTT TCT TTG GTC TGC ATT C-3 (reverse); for β-actin, 5 -TTC CTG GGC ATG GAG TCC T-3 (forward) and 5 -AGG AGG AGC AAT GAT CTT GAT C-3 (reverse). Real-time PCR reactions were carried out using a LightCycler FastStart DNA Master SYBR green I kit (Roche Molecular Biochemicals, Mannheim, Germany) as recommended by the manufacturer. Gene expression was quantified by dividing the level of HIF-1α and VEGF mRNA expression by the level of β-actin mRNA expression.

Analysis of HIF-1α and VEGF protein expression

Cells were seeded at a density of 2×10^5 cells/well in 6-well culture dishes, stimulated with TNFα and IL-1β as described above, and then incubated with FK228 (5 nM) under hypoxia for up to 24 h (0, 12, and 24 h). For analysis of HIF-1α, the cells were washed twice with PBS, scraped, and lysed, after which proteins were extracted in a buffer of ice-cold 1 % Triton X-100 in PBS supplemented with 1 mM PMSF, 2 mM *N*-ethylmaleimide, 5 mM iodoacetamide, and 1 mM EDTA. The resulting extract was incubated on ice for 5 min and centrifuged at 15,000 *g* for 10 min at 4 °C. The concentrations of proteins in the supernatant were measured and equalized using a Bio-Rad protein assay kit. Forty μg of protein per lane were run on 8 % SDS-PAGE gels and then transferred onto polyvinylidene difluoride membranes (Immobilon, Millipore, Bedford, MA). Membranes were blocked with 1 % bovine serum albumin (BSA) in PBS, incubated with primary antibody diluted in blocking so-

lution, washed with 0.05% Triton X-100 in PBS, and then incubated with the appropriate horseradish peroxidase (HRP)-conjugated secondary antibody diluted in blocking solution. Immuno-positive bands were detected using an enhanced chemiluminescence system (ECL, Amersham Phamacia Biotech). To confirm that the amounts of protein were equal, β-actin was run as an internal control.

Culture supernatants of RASFs were collected at each time point (0, 12, and 24 h) after FK228 (5 nM) treatment and kept frozen at –80 °C until analyzed. VEGF protein secreted into the culture media by RASFs was quantified using a human VEGF ELISA kit (R&D systems, Inc. Minneapolis, MN) according to the manufacturer's instructions. The values obtained from the experiments were adjusted to the total protein amounts in the culture media.

Induction of CAIA in mice

DBA/1 mice (Charles River Japan, Inc., Yokohama, Japan) were used to evaluate the *in vivo* effects of FK228 on VEGF expression in synovial tissue. All of the mice (n = 15) in the current study were 6- to 7-weeks-old. They were fed a standard commercial diet and tap water *ad libitum* at the Laboratory Animal Center for Biochemical Research, Okayama University Graduate School of Medicine and Dentistry, under standard diurnal conditions. Arthritis was induced by an arthritogenic cocktail of four monoclonal antibodies (mAbs) to type II collagen (Chondrex Inc, Redmond, WA) combined with LPS simulation according to the method of Terato et al. [29, 30]. DBA/1 mice were injected intravenously with 2 mg of mAbs on day 0 and day 1 (total 4 mg) followed by intraperitoneal injection of 50 μg LPS on day 2. After the onset of clinically distinct arthritis, FK228 was intravenously administrated once on day 4 at 2 mg/kg (n = 5). Control mice (n = 10) were injected with 10% HCO60 saline alone on the same day (day 4).

Clinical evaluation of arthritis

The mice were monitored for the development of arthritis every day after the first round of mAb injection. Arthritis was scored using a range of 0–4 points, according to the criteria of Terato et al. [29]. Each limb was graded individually, so that the maximum cumulative clinical arthritic score per mouse was 16 points.

Histological analysis of hind paws

The mice were euthanized by systemic perfusion with 4% paraformaldehyde under general anesthesia. Both hind limbs of CAIA mice before treatment (n = 5), CAIA mice without treatment (n = 5), and CAIA mice with FK228 treatment (n = 5) were dissected on day 4, 6, and 6, respectively, and fixed in the same solution for 24 h. The samples were decalcified by incubation in 0.3 M EDTA (pH 7.5) for 7–10 days, divided into two blocks in the sagittal plane, dehydrated in a graded series of ethanol, and embedded in paraffin. Hematoxylin and eosin staining, and Victoria-blue staining for elastic fibers of the blood vessels were performed on standard sagittal sections of 4.5 μm. The histology of the synovial inflammation as well as of the bone and cartilage damage was examined independently by two of the authors (KN and YN). The sections were blinded and graded according to the system described by Sancho et al. [31]: 0, no inflammation; 1, slight thickening of the synovial cell layer, and/or some inflammatory cells in the sublining; 2, thickening of the synovial lining, infiltration of the sublining, and localized cartilage erosions; and 3, infiltration of the synovial space, pannus formation, cartilage destruction, and bone erosion. The number of blood vessels stained by Victoria-blue within the field of 1 mm × 1 mm were counted in section of the tarsal joints of the hind limbs of normal mice without arthritis (n = 4), CAIA mice without treatment (n = 5) and CAIA mice with FK228 treatment (n = 5).

VEGF immunohistochemistry

The immunohistochemistry of VEGF was carried out as previously described [30], with the same series of paraffin sections used for the histological study. Endogenous peroxidase in the samples was blocked with 0.3% H_2O_2, Antigen was unmasked by treating the sections with 1 mg of hyaluronidase (*Streptomyces hyalurolyticus*) (Seikagaku Co., Tokyo, Japan) per ml for 1 h at room temperature. After non-specific binding had been blocked with 5% horse serum, the slides were incubated with polyclonal anti-VEGF antibody at 1: 100 overnight at 4 °C, and then with 7.5 μg biotinylated goat anti-rabbit IgG (Vector Laboratories Inc, CA) per ml for 30 min at room temperature. Histone Simple Stain MAX-PO (M) (Nichirei, Tokyo, Japan) and Simple Stain DAB solution (Nichirei) were used to visualize antibody binding. The sections were counterstained with hematoxylin. Negative control tissues were prepared in the same manner as described above, except for the omission of primary antibodies and the substitution of an isotype-matched but irrelevant antibody. The slides were blinded and scored by three independent observers (KN, YN, and HM) for VEGF staining using a 4-point scale: 0 = no staining, 1 = localized staining, 2 = widespread, but not total staining, and 3 = widespread, total staining of the synovial tissue. An average of the three observers' scores was determined, and the mean scores were statistically compared.

Statistical analysis

All RASF experiments were repeated at least three times and yielded similar results. Data were expressed as means ±SD. Statistical analysis was done using a one-way analysis of variance followed by either Fisher's least significant difference test or the Mann-Whitney *U* test, using Statview-J 5.0 software (SAS Institute, Cary, NC); $p < 0.05$ was considered statistically significant.

Results

FK228 inhibits the hypoxia-induced expression of HIF-1α and VEGF mRNA

The effects of FK228 on HIF-1α and VEGF mRNA expression in hypoxia-exposed RASFs were examined by quantitative real-time PCR. Neither hypoxia, FK228, nor a combination of both had an effect on cell morphology or cell survival during the 24-h experimental period (data not shown). FK228 down-regulated HIF-1α and VEGF mRNA expression under hypoxia in a dose-dependent manner (Fig. 1). Statistical analysis showed that 5 nM of FK228 was sufficient to inhibit the expression of HIF-1α and VEGF mRNA in RASFs. Under hypoxic conditions, HIF-1α expression was significantly up-regulated at 6 h ($p < 0.05$), and VEGF expression at 12 h ($p < 0.005$). Stimulation of the cells with IL-1β (1 ng/ml) and TNF-α (10 ng/ml) further enhanced HIF-1α expression at 12 and 24 h, and VEGF expression at 12 h ($p < 0.001$). Cytokine stimulation under hypoxia enhanced HIF-1α mRNA expression in a time-dependent manner; VEGF mRNA expression increased up to 12 h but decreased by 24 h. FK228 (5 nM) significantly down-regulated HIF-1α mRNA expression at 12 and 24 h (Fig. 2A), and VEGF mRNA expression at 12 and 24 h (Fig. 2B) ($p < 0.001$). The experiments for each condition were done at least three times and generated similar data. To study whether the down-regulation of HIF-1α and VEGF mRNA induced by FK228 was related to HDAC inhibition, the effect of trichostatin A (TSA), a classic HDAC inhibitor, was

examined. TSA also down-regulated the cytokine-induced expression of HIF-1α and VEGF mRNA under hypoxia (data not shown).

Effect of FK228 on HIF-1α and VEGF protein expression

The effect of FK228 (5 nM) on HIF-1α protein expression in RASFs was determined by Western blot analysis. The levels of HIF-1α protein increased under hypoxia in a time-dependent manner, whereas after incubation with FK228 (5 nM) the levels had decreased by 12 and 24 h (Fig. 3).

The effect of FK228 on the secretion of VEGF protein into the culture medium under hypoxia was also studied. VEGF secretion increased in a time-dependent manner under hypoxia (control) and was markedly up-regulated at 24 h following stimulation with IL-1β and TNFα. FK228 (5 nM) treatment significantly decreased VEGF secretion in the culture medium to a level below that of the control (Table 1).

Suppression of VEGF expression and inhibition of angiogenesis by FK228 in the synovial tissue of CAIA mice

By day 4, clinically apparent arthritis, with marked swelling or redness of the limb joints, had developed in all mice. We previously reported that the symptoms of clinical arthritis in mice treated with FK228 were barely apparent on day 10 and continued to diminish until the end of the observation period on day 15 [28]. Therefore, synovial tissue samples collected at day 4 and 6 were used for histological and immunohistochemical analyses of VEGF. The mean clinical scores of control and FK228-treated CAIA mice on day 6 were 12.6 ± 1.3 points, and 7.8 ± 1.3 points, respectively. There was a significant difference between the two groups ($p < 0.001$). Histologically, the hind-paw joint of control mice showed marked synovial proliferation and infiltration by inflammatory cells (Fig. 4A: a, b). The joint-inflammation score of control CAIA mice on day 4 and 6 were 0.9 ± 0.3, and 2.5 ± 0.5, respectively. In contrast, inflammation was less severe in the synovial tissue of FK228-treated mice. The joint inflammation score of the treated animals was 1.0 ± 0.7, which was significantly lower than that of control mice ($p < 0.001$; Fig. 4B). Intense staining for VEGF was noted in the synovial lining cells and in fibroblasts within the synovial tissue of control, non-treated mice. However, after treatment with FK228, VEGF expression significantly diminished (Fig. 4A: c, d). The VEGF staining scores of control CAIA mice on day 4, control CAIA mice on day 6, and FK228-treated mice on day 6 were 1.1 ± 0.8, 2.5 ± 0.7 and 1.1 ± 1.1, respectively. The score of FK228-treated mice was significantly lower than that of control mice ($p < 0.005$; Fig. 4C).

Victoria-blue staining successfully labeled the elastic fibers of blood vessels in the synovial tissue. The number of blood vessels within the field of normal mice without arthri-

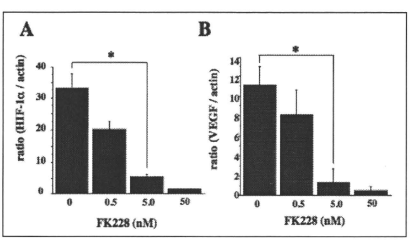

Fig. 1. Effects of various concentrations of FK228 on the expression of HIF-1α (**A**) and VEGF (**B**) mRNA. Cells were stimulated with IL-1β and TNFα for 1 h and then placed under hypoxic condition (1 % O_2) for 24 h. FK228 down-regulated the expression of HIF-1α and VEGF in a dose-dependent manner as shown by quantitative real-time PCR. Results were reproducible in repeated experiments. *$p < 0.001$ versus vehicle treatment

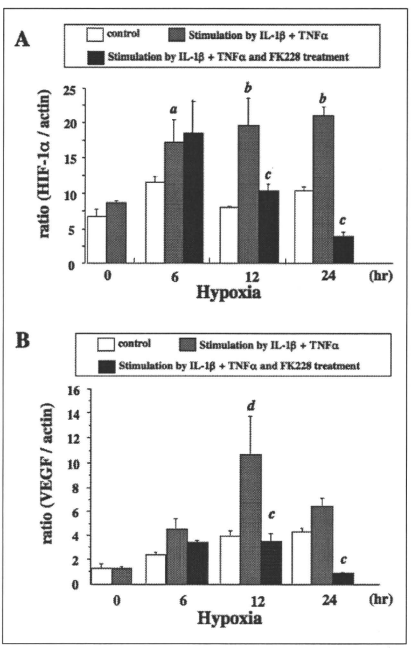

Fig. 2. Time course of the effects of FK228 on the expression of HIF-1α (**A**) and VEGF (**B**) mRNA. Cells were stimulated with IL-1β and TNFα for 1 h and then placed under hypoxic conditions (1 % O_2) for 24 h with or without FK228 (5 nM). Hypoxia up-regulated HIF-1α and VEGF expression for up to 24 h. IL-1β and TNFα stimulation further enhanced the expression of HIF-1α and VEGF mRNA under hypoxia. FK228 (5 nM) effectively countered the cytokine-enhanced up-regulation of HIF-1α and VEGF after 12 h. *a*: $p < 0.05$, *b*: $p < 0.005$, *d*: $p < 0.001$ vs. control, and *c*: $p < 0.001$ vs. stimulation by IL-1β+TNFα without FK228 treatment.

tis, control CAIA mice on day 6, and FK228-treated mice on day 6 were 9.8 ± 2.2, 19.0 ± 3.4, and 12.2 ± 1.3, respectively. The number of blood vessels of FK228-treated mice was significantly lower than that of control mice ($p < 0.001$; Fig. 5).

Discussion

We recently demonstrated that FK228, a specific inhibitor of HDAC, prevents the *in vitro* proliferation of RASFs and ameliorates the pathological changes of autoantibody-mediated arthritis in mice. Furthermore, we also showed that the effects of FK228 are controlled, at least in part, by the regulation of $p16^{INK4a}$ and $p21^{Cip1/WAF1}$ gene expression [28]. The results strongly suggested that modulation of the transcriptional activity of specific promoters in response to the local release or perturbation of chromatin structure, by treatment with HDAC inhibitor, could effectively prevent the synovial proliferation and joint destruction seen in human RA. Nonetheless, the inhibitory effects on cell cycle regulation and cell proliferation were not sufficient to explain the strong anti-inflammatory effects of HDAC inhibitor that are exerted *in vivo*. Interestingly, several recent studies indicated that the inhibitory property of FK228 on hypoxia-induced angiogenesis occurred via suppression of both HIF-1α activity and VEGF mRNA expression [26, 27, 32]. As VEGF plays a central role in the angiogenic process in RA, we investigated the effects of FK228 on HIF-1α and VEGF expression in RASFs. Our results showed that, in response to hypoxia and stimulation with pro-inflammatory cytokines, FK228 inhibited both the expression of HIF-1α and the induction of VEGF in RASFs at the mRNA and protein levels. The present study further demonstrated that intravenous administration of FK228 (2.5 mg/kg) effectively ameliorated joint inflammation and suppressed VEGF expression in the synovial tissue of CAIA mice on day 6. Semi-quantitative analysis on the number of blood vessels in the synovial tissue

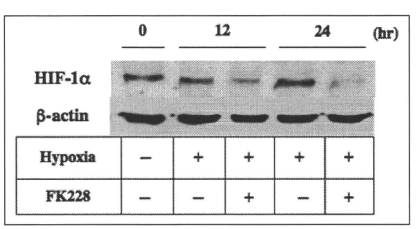

Fig. 3. Results of Western blot analysis of HIF-1α protein expression. Cells were stimulated with IL-1β and TNFα for 1 h and then placed under hypoxic conditions (1 % O_2) either with or without FK228 (5 nM) for 24 h. Samples were taken at the indicated time points and HIF-1α protein levels were analyzed by Western blotting. FK228 (5 nM) effectively repressed HIF-1α expression under hypoxia. The experiment was repeated three times with similar results.

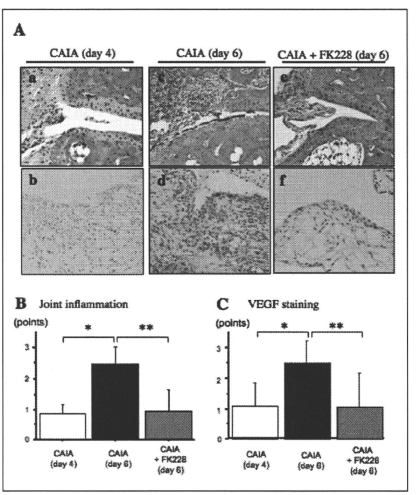

Fig. 4. *In vivo* effect of FK228 on joint inflammation and VEGF expression in the hind-paw joints of CAIA mice. (**A**) Representative histological appearances of hind-paw joints, stained with hematoxylin and eosin (H.E.) (a, c, e) and immunohistochemistry for VEGF (b, d, f) of the synovial tissue of in control CAIA mice on day 4 (*a, b*), control CAIA mice on day 6 (c, d), and FK228-treated CAIA mice on day 6 (e, f). (**B**) Histological scores of joints on day 4 and 6 in control and on day 6 in FK228 (2.5 mg/kg) treatment groups (*$p < 0.01$). (**C**) Scores of VEGF staining of the synovial tissue of control and treatment mice (*$p < 0.001$, **$p < 0.005$). *Error bars* indicate standard errors of the means.

Table 1. Effects of FK228 (5 nM) on hypoxia- and cytokine-induced VEGF secretion by rheumatoid synovial fibroblasts into the culture media (pg/well)

Hypoxia (hr)	control	IL-1β + TNFα	
		FK228 (–)	FK228 (+)
0	N. D.	N. D.	N. D.
12	641.1 ± 4.8	1125.4 ± 105.6	389.4 ± 21.2*
24	1763.5 ± 351.0	14312.1 ± 2561.0	952.7 ± 30.0*

N. D.: not detected, *: $p < 0.001$

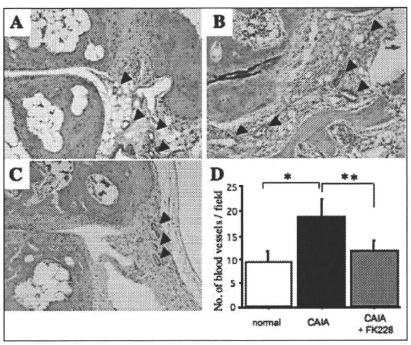

Fig. 5. Effects of FK228 on the angiogenesis in the synovial tissue of CAIA mice. A–C: staining of the synovial tissue of hind limb joints from normal mice without arthritis (A Victoria-blue), CAIA mice without treatment at day 6 (B), and CAIA mice treated with FK228 at day 6 (C). Arrow heads: blood vessels stained by Victoria blue, original magnification: ×100. D: Number of Victoria-blue-stained blood vessels in the synovial tissue in each group of mice ($*p < 0.001$, $**p < 0.005$). *Error bars* indicate standard errors of the means.

stained by Victoria-blue staining demonstrated the blockage of angiogenesis by FK228. These findings suggest that the modification of chromatin structure by HDAC inhibitors plays a beneficial role in the control of synovial angiogenesis via regulation of hypoxia-regulated genes.

The mechanism of the inhibitory effect on HIF-1α and VEGF expression by HDAC inhibitors is not fully understood. In the current study, the effect of HDAC inhibition by FK228 on HIF-1α expression was not apparent until 12 h. In HepG2 human hepatoblastoma cells, hypoxia-induced HDAC activity responded in a time-dependent manner, reaching a maximum at 16 hours [25]. The overexpression of wild-type HDAC1 in HepG2 cells resulted in significant up-regulations of HIF-1α and VEGF mRNA [25]. These results suggest that the effect of FK228 on HIF-1α and VEGF mRNA might be partly exhibited by the direct inhibition of hypoxia-induced HDAC activity in RASF.

It is not still clear whether histone acetylation by HDAC inhibitors selectively modulates the expression of these genes under hypoxic conditions [32]. Lee et al. demonstrated that FK228 inhibited the hypoxia-induced expression and DNA-binding activity of HIF-1α in Lewis lung carcinoma cells. The direct effect of FK228 on HIF-1 activity was suggested to prohibit VEGF induction in response to hypoxia, thereby inhibiting tumor angiogenesis [32]. Sasakawa et al. reported histone acetylation of VEGF promoter regions and suppression of VEGF gene expression by FK228 in PC-3 prostate cancer cells. The authors speculated that the patterns of histone acetylation of VEGF differed from those involved in the up-regulation of gene expression. It was also suggested that the alterations in chromatin structure induced by FK228-mediated histone acetylation result in the failure of transcription-factor binding to VEGF gene promoters [27]. In RA joints, RASFs spontaneously release proinflammatory cytokines, such as IL-1, IL-6, IL-8, TGFβ, TNFα, all of which are potent inducers of angiogenesis in vivo [8, 9]. A variety of cytokines, including IL-1β and TNFα, are known to stabilize and activate HIF-1α [33, 34]. Stimulation of cultured RASFs by IL-1β increased HIF-1α mRNA levels as well as the binding of the heterodimer HIF-1 to the HIF consensus sequence [33]. IL-1β and TNF α stimulated HIF-1 binding to DNA in human hepatoma cells [34]. In the current study, the up-regulation of HIF-1α mRNA expression seen after 6 h stimulation might be mainly induced by exogenous IL-1β and TNFα without requiring *de novo* protein synthesis, because hypoxic regulation of HIF-1α occurs at the post-translational level by protein stabilization [33]. Among the HIF-1-inducible genes, only VEGF has been shown to be induced by IL-1β and TNF-α in RASFs [1, 33]. The fact that the effect of IL-1 on HIF-1 DNA-binding activity was not fully apparent until 6 hours stimulation in human synovial fibroblasts [33] might reasonably explain the relatively delayed up-regulation of cytokin-induced VEGF mRNA expression to HIF-1 expression at 12 h seen in the current study. Furthermore, we demonstrated that FK228 inhibited the expression of IL-1β and TNF-α in the synovium of CAIA mice in a previous study [28]. Thus, it is possible that down-regulation of VEGF expression *in vivo* at 12 h might be induced by down-regulation of not only HIF-1α expression, but by suppression of endogenous IL-1β and TNF-α expression following FK228 treatment.

Another explanation for the down-regulation of VEGF gene expression by HDAC inhibition may be that HDAC inhibitors inactivate transcriptional factors other than HIF-1 by modifying the activities of cell cycle regulators. HDAC inhibitors are known to exert anti-arthritic properties by up-regulation of $p21^{Cip1/WAF1}$, a cyclin-dependent kinase (CDK) inhibitor, via acetylation of promoter regions of the gene [28, 35]. Recent report demonstrated that adenoviral $p21^{Cip1/WAF1}$ gene transfer into RASF resulted in the inhibition of inflammatory gene expression by reducing the activity of c-Jun NH_2-terminal kinase (JNK), which phosphorylates the c-Jun component of AP-1 transcriptional factor [36, 37], or by inactivation of the transcription factor NF-κB [34]. The entire complex of AP-1 and HIF-1 contributes to the activation and expression of VEGF under hypoxic conditions. In addition, NF-κB is strongly activated by reoxygenation and is involved in the up-regulation of many inflammatory genes, including VEGF [38]. Taken together, these findings suggest that HDAC-inhibitor-induced up-regulation of $p21^{Cip1/WAF1}$ contributes to the inhibition of VEGF expression via inactivation of NF-κB and/or AP-1 in hypoxic RASFs.

In conclusion, we have demonstrated that FK228 down-regulates the expression of hypoxia-induced HIF-1α and VEGF in RASF. Similarly, VEGF expression and number of blood vessels in synovial tissues decreased in the joints of CAIA mice treated by systemic administration of FK228. Further studies aimed at exploring the precise, HDAC-specific mechanisms underlying the regulation of oxygen-dependent gene expression and hypoxia-induced angiogenesis in RA are needed.

Acknowledgement. We thank Dr. S Hirohata and Dr. T Yonezawa, Department of Molecular Biology and Biochemistry, and Dr. Akihiro Matsukawa, Department of Pathology and Experimental Medicine, Okayama

University Graduate School of Medicine, Dentistry and Pharmateutical Sciences, for generous technical assistance. The authors also thank Mrs. C. McCown for editing the manuscript. This work was supported by a grant from the Japan Orthopaedics and Traumatology Foundation, Inc, No. 148.

References

[1] Paleolog EM, Young S, Stark AC, McCloskey RV, Feldmann M, Maini RN. Modulation of angiogenic vascular endothelial growth factor by tumor necrosis factor α and interleukin-1 in rheumatoid arthritis. Arthritis Rheum 1998; 41: 1258–65.

[2] Lund-Olesen K. Oxygen tension in synovial fluids. Arthritis Rheum 1970; 13: 769–76.

[3] Walsh DA, Haywood L. Angiogenesis: a therapeutic target in arthritis. Curr Opin Investig Drugs 2001; 2: 1054–63.

[4] Schrieber L, Jackson CJ. Angiogenesis in rheumatoid arthritis. In: Klippel JH, Dieppe PA et al, editors. Rheumatology. London: Mosby; 1998. Section 5,12.1–4.

[5] Josko J, Mazurek M. Transcription factors having impact on vascular endothelial growth factor (VEGF) gene expression in angiogenesis. Med Sci Monit 2004; 10: RA89–98.

[6] Koch AE, Harlow LA, Haines GK, Amento EP, Unemori EN, Wong WL et al. Vascular endothelial growth factor. A cytokine modulating endothelial function in rheumatoid arthritis. J Immunol 1994; 152: 4149–56.

[7] Fava RA, Olsen NJ, Spencer-Green G, Yeo Kt, Yeo TK, Berse B et al. Vascular permeability factor/endothelial growth factor (VPF/VEGF): accumulation and expression in human synovial fluids and rheumatoid synovial tissue. J Exp Med 1994; 180: 341–6.

[8] BenEzra D. Neovasculogenic ability of prostaglandins, growth factors, and synthetic chemoattractants. Am J Ophthalmol 1978; 86: 455–61.

[9] BenEzra D, Hemo I, Maftzir G. In vivo angiogenic activity of interleukins. Arch Ophthalmol 1990; 108: 573–6.

[10] Peacock DJ, Banquerigo ML, Brahn E. Angiogenesis inhibition suppresses collagen arthritis. J Exp Med 1992; 175: 1135–8.

[11] Firestein GS. Starving the synovium: angiogenesis and inflammation in rheumatoid arthritis. J Clin Invest 1999; 103: 3–4.

[12] Folkman J. Angiogenesis. In: Smolen JS, Lipsky PE, eds. Targeted therapies in rheumatology. London: Martin Dunitz; 2003, p. 111–30.

[13] Hitchon C, Wong K, Ma G, Reed J, Lyttle D, El-Gabalawy H. Hypoxia-induced production of stromal cell-derived factor 1 (CXCL12) and vascular endothelial growth factor by synovial fibroblasts. Arthritis Rheum 2002; 46: 2587–97.

[14] Giatromanolaki A, Sivridis E, Maltezos E, Athanassou N, Papazoglou D, Gatter KC et al. Upregulated hypoxia inducible factor-1α and -2α pathway in rheumatoid arthritis and osteoarthritis. Arthritis Res Ther 2003; 5: R193–201.

[15] Makino Y, Nakamura H, Ikeda E, Ohnuma K, Yamauchi K, Yabe Y et al. Hypoxia-inducible factor regulates survival of antigen receptor-driven T cells. J Immunol 2003; 15: 6534–40.

[16] Grunstein M. Histone acetylation in chromatin structure and transcription. Nature 1997; 389: 349–52.

[17] Kuo MH, Allis CD. Roles of histone acetyltranferases and deacetylases in gene regulation. Bioessays 1998; 20: 615–26.

[18] Hassing CA, Schreiber SL. Nuclear histone acetylases and deacetylases and transcriptional regulation: HATs off to HDACs. Curr Opin Chem Biol 1997; 1: 300–8.

[19] Byrd JC, Shinn C, Ravi R, Willis CR, Waselenko JK, Flinn IW et al. Desipeptide (FR901228): a novel therapeutic agent with selective, in vitro activity against human B-cell chronic lymphocytic leukemia cells. Blood 1999; 94: 1401–8.

[20] Nakajima H, Kim YB, Terano H, Yoshida M, Horinouchi S. FR901228, a potent antitumor antibiotic, is a novel histone deacetylase inhibitor. Exp Cell Res 1998; 241: 126–33.

[21] Huang L, Pardee AB. Suberoylanilide hydroxamic acid as a potential therapeutic agent for human breast cancer treatment. Mol Med 2000; 6: 849–66.

[22] Kosugi H, Towatari M, Hatano S, Kitamura K, Kiyoi H, KinoshitaT et al. Histone deacetylase inhibitors are the potent inducer / enhancer of differentiation in acute myeloid leukemia: a new approach to anti-leukemia therapy. Leukemia 1999; 13: 1316–24.

[23] Ferrara FF, Fazi F, Bianchini A, Padula F, Gelmetti V, Minucci S, Mancini M, Pelicci PG, Lo Coco F, Nervi C. Histone deacetylase-targeted treatment restores retinoic acid signaling and differentiation in acute myeloid leukemia. Cancer Res 2001; 61: 2–7.

[24] Kwon HJ, Owa T, Hassig CA, Shimada J, Schreiber SL. Depudecin induces morphological reversion of transformed fibroblasts via the inhibition of histone deacetylase. Proc Natl Acad Sci USA 1998; 95: 3356–61.

[25] Kim MS, Kwon HJ, Lee YM, Baek JH, Jang JE, Lee SW et al. Histone deacetylases induce angiogenesis by negative regulation of tumor suppressor gene. Nat Med 2001; 7: 437–43.

[26] Kwon HJ, Kim MS, Kim MJ, Nakajima H, Kim KW. Histone deacetylase inhibitor FK228 inhibits tumor angiogenesis. Int J Cancer 2002; 97: 290–6.

[27] Sasakawa Y, Naoe Y, Noto T, Inoue T, Sasakawa T, Matsuo M et al. Antitumor efficacy of FK228, a novel histone deacetylase inhibitor, depends on the effect on expression of angiogenesis factors. Biochem Pharmacol. 2003; 66: 897–906.

[28] Nishida K, Komiyama T, Miyazawa S, Shin ZN, Furumatsu T, Doi H et al. Histone deacetylase inhibitor suppression of autoantibody-mediated arthritis in mice via regulation of $p16^{INK4a}$ and $p21^{WAF/Cip1}$ expression. Arthritis Rheum 2004; 50: 3365–76.

[29] Terato K, Hasty KA, Reife RA, Cremer MA, Kang AH, Stuart JM. Induction of arthritis with monoclonal antibodies to collagen. J Immunol 1992; 148: 2103–8.

[30] Kato H, Nishida K, Yoshida A, Takada I, McCown C, Matsuo M et al. Effect of NOS2 gene deficiency on the development of autoantibody mediated arthritis and subsequent articular cartilage degeneration. J Rheumatol 2003; 30: 247–55.

[31] Sancho D, Gomez M, Viedma F, Esplugues E, Gordon-Alonso M, Garcia-Lopez MA et al. CD69 downregulates autoimmune reactivity through active transforming growth factor- production in collagen-induced arthritis. J Clin Invest 2003; 112: 872–82.

[32] Mie Lee Y, Kim SH, Kim HS, Jin Son M, Nakajima H, Jeong Kwon H et al. Inhibition of hypoxia-induced angiogenesis by FK228, a specific histone deacetylase inhibitor, via suppression of HIF-1α activity. Biochem Biophs Res Commun 2003; 300: 241–6.

[33] Thornton RD, Lane P, Borghaei RC, Pease EA, Caro J, Mochan E. Interleukin 1 induces hypoxia-inducible factor 1 in human gingival and synovial fibroblasts. Biochem J 2000; 350: 307–12.

[34] Hellwig-Bürgel T, Rutkowski K, Metzen E, Fandrey J, Jelkmann W. Interleukin-1beta and tumor necrosis factor-alpha stimulate DNA binding of hypoxia-inducible factor-1. Blood 1999; 94: 1561–7.

[35] Chung YL, Lee MY, Wang AJ, Yao LF. A Therapeutic strategy uses histone deacetylase inhibitors to modulate the expression of genes involved in the pathogenesis of rheumatoid arthritis. Mol Ther 2003; 8: 707–17.

[36] Nonomura Y, Kohsaka H, Nagasaka K, Miyasaka N. Gene transfer of a cell cycle modulator exerts anti-inflammatory effects in the treatment of arthritis. J Imumunol 2003; 171: 4913–9.

[37] Perlman H, Bradley K, Liu H, Cole S, Shamiyeh E, Smith RC et al. IL-6 and matrix metalloproteinase-1 are regulated by the cyclin-dependent kinase inhibitor p21 in synovial fibroblasts. J Immunol. 2003; 170: 838–45.

[38] Muller JM, Rupec RA, Baeuerle PA. Study of gene regulation by NF-κB and AP-1 in response to reactive oxygen intermediates. Methods 1997; 11: 301–12.

ARTHRITIS & RHEUMATISM
Vol. 58, No. 5, May 2008, pp 1284–1292
DOI 10.1002/art.23429
© 2008, American College of Rheumatology

Expression of MicroRNA-146 in Rheumatoid Arthritis Synovial Tissue

Tomoyuki Nakasa,[1] Shigeru Miyaki,[2] Atsuko Okubo,[1] Megumi Hashimoto,[2] Keiichiro Nishida,[3] Mitsuo Ochi,[4] and Hiroshi Asahara[5]

Objective. **Several microRNA, which are ~22-nucleotide noncoding RNAs, exhibit tissue-specific or developmental stage–specific expression patterns and are associated with human diseases. The objective of this study was to identify the expression pattern of microRNA-146 (miR-146) in synovial tissue from patients with rheumatoid arthritis (RA).**

Methods. **The expression of miR-146 in synovial tissue from 5 patients with RA, 5 patients with osteoarthritis (OA), and 1 normal subject was analyzed by quantitative reverse transcription–polymerase chain reaction (RT-PCR) and by in situ hybridization and immunohistochemistry of tissue sections. Induction of miR-146 following stimulation with tumor necrosis factor α (TNFα) and interleukin-1β (IL-1β) of cultures of human rheumatoid arthritis synovial fibroblasts (RASFs) was examined by quantitative PCR and RT-PCR.**

Results. **Mature miR-146a and primary miR-146a/b were highly expressed in RA synovial tissue, which also expressed TNFα, but the 2 microRNA were less highly expressed in OA and normal synovial tissue. In situ hybridization showed primary miR-146a expression in cells of the superficial and sublining layers in synovial tissue from RA patients. Cells positive for miR-146a were primarily CD68+ macrophages, but included several CD3+ T cell subsets and CD79a+ B cells. Expression of miR-146a/b was markedly upregulated in RASFs after stimulation with TNFα and IL-1β.**

Conclusion. **This study shows that miR-146 is expressed in RA synovial tissue and that its expression is induced by stimulation with TNFα and IL-1β. Further studies are required to elucidate the function of miR-146 in these tissues.**

Rheumatoid arthritis (RA) is characterized by chronic inflammation of synovial tissue, causing destruction of cartilage and bone (1). Synovial tissue from RA patients shows infiltration by macrophages, T cells, and B cells, proliferation of the lining cells, and production of inflammatory cytokines, such as tumor necrosis factor α (TNFα) and interleukin-1β (IL-1β). Inhibiting these cytokines ameliorates clinical symptoms, which strongly supports the important roles played by cytokines in RA (2,3).

The transcription factor NF-κB is a key regulator of inflammation (4,5). Several studies have revealed that activated NF-κB is detected in RA synovial tissue, and its expression contributes to the initiation and maintenance of chronic inflammation (6–8). Not only does NF-κB regulate the expression of the inflammatory cytokines TNFα and IL-1β, but it also promotes the secretion of IL-2, IL-12, and interferon-γ (IFNγ) from Th1 cells, which subsequently activates macrophages. In addition, NF-κB activation promotes synovial hyperplasia by stimulating cell proliferation and inhibiting *c-myc*–induced apoptosis (9,10).

MicroRNA are a family of ~22-nucleotide non-

Supported by the NIH (grants AR-50631 and AR-47360), the Arthritis Foundation, the Japan Science and Technology Agency SORST Project, the Japanese National Institute of Biomedical Innovation, Genome Network Project (MEXT), and DECODE.

[1]Tomoyuki Nakasa, MD, PhD, Atsuko Okubo, MS: National Research Institute for Child Health and Development, Tokyo, Japan, and Hiroshima University Graduate School of Biomedical Sciences, Hiroshima, Japan; [2]Shigeru Miyaki, PhD, Megumi Hashimoto, MD, PhD: National Research Institute for Child Health and Development, Tokyo, Japan; [3]Keiichiro Nishida, MD, PhD: Okayama University Graduate School of Medicine and Dentistry, Okayama, Japan; [4]Mitsuo Ochi, MD, PhD: Hiroshima University Graduate School of Biomedical Sciences, Hiroshima, Japan; [5]Hiroshi Asahara, MD, PhD: National Research Institute for Child Health and Development, Tokyo, Japan, and Scripps Research Institute, La Jolla, California.

Drs. Nakasa and Miyaki contributed equally to this work.

Address correspondence and reprint requests to Hiroshi Asahara, MD, PhD, Department of Regenerative Biology and Medicine, National Research Institute for Child Health and Development, Research Institute, 2-10-1 Okura, Setagaya, Tokyo 157-8535, Japan. E-mail: asahara@nch.go.jp.

Submitted for publication May 9, 2007; accepted in revised form January 28, 2008.

Table 1. Demographic and clinical features of the study subjects*

Subject/age/sex	Disease duration, years	Larsen score for RA	K/L score for OA	CRP level presurgery, mg/liter	Source of synovium	Medication
RA patients						
RA1/59/F	14	IV	–	0.63	Wrist	Pred. 4.5 mg/day
RA2/38/F	12	IV	–	2.3	Knee	Pred. 5.0 mg/day
RA3/64/F	28	IV	–	0.5	Knee	Pred. 5.0 mg/day; SSZ 1 gm/day
RA4/75/F	22	IV	–	0.31	Elbow	Pred. 10 mg/day
RA5/58/F	9	IV	–	0.69	Knee	Pred. 3.0 mg/day; MTX 5 mg/week
OA patients						
OA6/68/F	–	–	IV	0	Knee	NSAIDs
OA7/65/F	–	–	IV	0.7	Knee	NSAIDs
OA8/71/F	–	–	IV	0	Knee	None
OA9/71/F	–	–	IV	0	Knee	NSAIDs
OA10/76/F	–	–	IV	0	Knee	NSAIDs
Normal subject						
11/55/M	–	–	–	–	Knee	–

* RA = rheumatoid arthritis; K/L = Kellgren/Lawrence; OA = osteoarthritis; CRP = C-reactive protein; Pred. = prednisolone; SSZ = sulfasalazine; MTX = methotrexate; NSAIDs = nonsteroidal antiinflammatory drugs.

coding RNAs identified in organisms ranging from nematodes to humans (11–13). Many microRNA are evolutionarily conserved across phyla, regulating gene expression by posttranscriptional gene repression. Long primary transcripts (primary microRNA) are transcribed by RNA polymerase II, processed by the nuclear enzyme Drosha, and released as an ~60-bp hairpin precursor micro. Precursor microRNA are processed by the RNase III enzyme Dicer to ~22 nucleotides (mature microRNA) and then incorporated into RNA-induced silencing complex (RISC). The microRNA–RISC complex binds the 3′-untranslated region of target messenger RNA (mRNA) and either promotes translational repression or mRNA degradation (14–17). Several microRNA exhibit a tissue-specific or developmental stage–specific expression pattern and have been reported to be associated with conditions such as cancer and viral infection (18,19).

Taganov et al (20) reported that microRNA-146a/b (miR-146a/b) is induced in response to lipopolysaccharide (LPS) and proinflammatory mediators and that miR-146a induction is regulated by NF-κB. They also found that miR-146a/b targets were TNF receptor–associated factor 6 (TRAF6) and IL-1 receptor–associated kinase 1 (IRAK1) genes and concluded that miR-146 plays a role in fine-tuning innate immune responses by negative feedback, including down-regulation of TRAF6 and IRAK1 genes.

Until now, there has been no report of miR-146 expression in human disease. RA is a representative inflammatory disease involving proinflammatory cytokines, such as TNFα and IL-1β. We therefore sought to determine whether miR-146 is expressed in RA synovial tissue.

PATIENTS AND METHODS

Patients and controls. Five patients who fulfilled the American College of Rheumatology (formerly, the American Rheumatism Association) classification criteria for RA (21) were included. Their clinical characteristics are shown in Table 1. All RA patients were treated with low-dose corticosteroids; 2 of the patients (RA3 and RA5) were also treated with the disease-modifying antirheumatic drugs (DMARDs) methotrexate and sulfasalazine, respectively. Patient RA3 had mutilating disease, with severe joint destruction. Patient RA5 showed more erosive disease, with severe destruction in the large joints. Patients RA1 and RA4 had the least erosive disease. The disease in patient RA1 was well controlled, and severe joint destruction was localized to the small joints of the wrists and feet. Patient RA4 had end-stage joint destruction, accompanied by vasculitis; the vasculitis was controlled with 10 mg of corticosteroids per day. Patient RA2 had more erosive disease, but was treated with steroids only because she was trying to become pregnant; thus, in this patient, disease control was poor and joint destruction severe.

In addition, 5 patients with knee osteoarthritis (OA) diagnosed according to typical clinical features and 1 patient undergoing leg amputation, but whose knee joint was normal, were included. All OA synovial tissue samples were obtained by total knee arthroplasty.

Clinical research was conducted in compliance with the Declaration of Helsinki. Written permission was obtained from all subjects who participated in the study.

Tissue samples. Synovial tissue was obtained from 5 patients with RA and 5 patients with OA who were undergoing open synovectomy or total joint replacement, as well as from a patient with a normal joint who was undergoing above-the-knee amputation because of angiosarcoma (Table 1). Three

synovial tissue specimens were obtained from random sites during surgery. Each sample was inspected visually to ensure that only inflamed tissue was included. Tissue samples were stored at –70°C until analyzed.

For polymerase chain reaction (PCR) analysis, total RNA was isolated from tissue samples that had been homogenized on ice with Isogen reagent (Nippon Gene, Toyama, Japan). For histopathologic analysis, the tissue samples were fixed in 4% paraformaldehyde and embedded in paraffin.

Synthesis of complementary DNA (cDNA). One microgram of total RNA was reverse-transcribed using 0.5 $\mu g/\mu l$ of oligo(dT) primer and First-Strand Reaction Mix Beads (GE Healthcare, Little Chalfont, UK). The reaction mixture was incubated for 60 minutes at 37°C.

Quantitative (real-time) PCR. Quantitative reverse transcription–PCR (RT-PCR) assays were performed using a TaqMan microRNA assay kit (Applied Biosystems, Foster City, CA) for the mature microRNA and using SYBR Green (Applied Biosystems) for the primary miR-146a/b and TNFα. RT reactions of mature microRNA contained a sample of total RNA, 50 n*M* stem-loop RT primer, 10× RT buffer, 100 m*M* each dNTPs, 50 units/μl of MultiScribe reverse transcriptase, and 20 units/μl of RNase inhibitor. Reaction mixtures (15 μl) were incubated in a thermocycler (Applied Biosystems) for 30 minutes at 16°C, 30 minutes at 42°C, and 5 minutes at 85°C and then maintained at 4°C.

Real-time PCR was performed using an Applied Biosystems 7900HT Sequence Detection System in a 10-μl PCR mixture containing 1.33 μl of RT product, 2× TaqMan Universal PCR Master Mix, 0.2 μM TaqMan probe, 15 μM forward primer, and 0.7 μM reverse primer. Each SYBR Green reaction was performed with 1.0 μl of template cDNA, 10 μl of SYBR Green mixture, 1.5 μM primer, and water to adjust the final volume to 20 μl.

Primer sequences were as follows: for primary miR-146a, 5′-CAG-CTG-CAT-TGG-ATT-TAC-CA-3′ (forward) and 5′-GCC-TGA-GAC-TCT-GCC-TTC-TG-3′ (reverse); for primary miR-146b, 5′-AGA-CCC-TCC-CTG-GAA-TAG-GA-3′ (forward) and 5′-CAC-CTG-GCT-GGG-AAG-TTG-3′ (reverse); for TNFα, 5′-GAG-TGA-CAA-GCC-TGT-AGC-CCA-3′ (forward) and 5′-AGC-TCC-ACG-CCA-TTG-GC-3′ (reverse); and for GAPDH, 5′-CAT-TGG-CAA-TGA-GCG-GTT-C-3′ (forward) and 5′-GGT-AGT-TTC-GTG-GAT-GCC-ACA-3′ (reverse). All reactions were incubated in a 96-well plate at 95°C for 10 minutes, followed by 40 cycles of 95°C for 15 seconds, and 60°C for 1 minute; all were performed in triplicate. The let-7a or GAPDH gene was used as a control to normalize differences in total RNA levels in each sample. A threshold cycle (C_t) was observed in the exponential phase of amplification, and quantification of relative expression levels was performed using standard curves for target genes and the endogenous control. Geometric means were used to calculate the $\Delta\Delta C_t$ values and were expressed as $2^{-\Delta\Delta C_t}$. The value of each control sample was set at 1 and was used to calculate the fold change in target genes.

Histologic analysis and in situ hybridization. Paraffin-embedded tissue was sectioned at 5 μm and stained with hematoxylin and eosin. For in situ hybridization, primary miR-146a fragments were derived from PCR products, cloned using the Qiagen PCR cloning kit into the pDrive vector (Qiagen, Chatsworth, CA), and sequenced. Primer sequences for primary miR-146a were 5′-TAT-TGG-GCA-AAC-AAT-CAG-CA-3′ (forward) and 5′-GCC-TGA-GAC-TCT-GCC-TTC-TG-3′ (reverse).

Digoxigenin (DIG)–labeled riboprobes were transcribed with a DIG RNA labeling kit and T7 polymerase (Roche, Mannheim, Germany). After deparaffinization, each section was fixed in 4% paraformaldehyde for 10 minutes at room temperature, washed 3 times in phosphate buffered saline (PBS) for 3 minutes, and subsequently treated with 600 μg of proteinase K for 10 minutes at room temperature. After treatment in 0.2% glycine-PBS for 10 minutes, sections were refixed in 4% paraformaldehyde for 10 minutes, washed 3 times in PBS for 3 minutes each, and acetylated with 0.25% acetic anhydride in 0.1*M* triethanolamine hydrochloride for 10 minutes. After washing in PBS for 30 minutes, sections were prehybridized for 1 hour at 65°C with prehybridization buffer (50% formamide and 5× saline–sodium citrate [SSC]). Hybridization with DIG-labeled riboprobes was performed overnight at 65°C in hybridization buffer (50% formamide, 5× SSC, 5× Denhardt's solution, and 250 μg/ml of Baker's yeast transfer RNA). After hybridization, sections were washed in 5× SSC for 30 minutes at 65°C, 0.2× SSC for 2 hours at 65°C, and 0.2× SSC for 5 minutes at room temperature. Blocking was performed overnight at 4°C with 4% horse serum and alkaline phosphatase–conjugated Fab anti-DIG antibody (Roche) in 1% sheep serum. Staining was performed using BCIP and nitroblue tetrazolium (NBT; Roche).

Double staining combining in situ hybridization and immunohistochemistry. Sections stained with BCIP and NBT and washed in PBS were treated for 20 minutes at 90°C with retrieval solutions (Nakalaitesque, Tokyo, Japan). After blocking for 30 minutes with blocking reagent (Nakalaitesque), sections were incubated with primary antibody at appropriate dilutions for 1 hour at room temperature. For primary antibodies, monoclonal mouse anti-human antibody against CD68 (Dako, Carpentaria, CA) and CD3ε (BD PharMingen, San Diego, CA), and monoclonal rabbit anti-human antibody against CD79a (Spring Bioscience, Fremont, CA) were used. After washing, sections were incubated with Alexa Fluor 594 conjugate for CD68 and CD3, and with Alexa Fluor 569 conjugate for CD79a (Invitrogen, Carlsbad, CA) for 30 minutes at room temperature, washed, and then incubated with 4′,6-diamidino-2-phenylindole (Dojindo Laboratories, Kumamoto, Japan). The negative control was prepared in the same manner, but without the primary antibody.

Isolation and culture of human RA synovial fibroblasts (RASFs). Fresh synovial tissue was obtained from a separate group of 4 RA patients. Synovial cells were isolated from the synovial tissue and cultured as described elsewhere (22). After the third passage, cells appeared to be morphologically homogeneous fibroblast-like cells. RASFs at passages 4–6 were used for the experiments.

Induction of miR-146a expression in RASFs by TNFα and IL-1β. Cells were seeded at 1.0×10^5/well into a 6-well plate containing 2 ml of Dulbecco's modified Eagle's medium plus 10% fetal bovine serum and 1% penicillin/streptomycin. After cells became adherent, they were treated with both recombinant human TNFα (1 ng/ml) and IL-1β (10 ng/ml) (R&D Systems, Minneapolis, MN) and then incubated for 24 hours under an atmosphere of 5% CO_2. Cells were washed twice with cold PBS, and then total RNA was isolated with

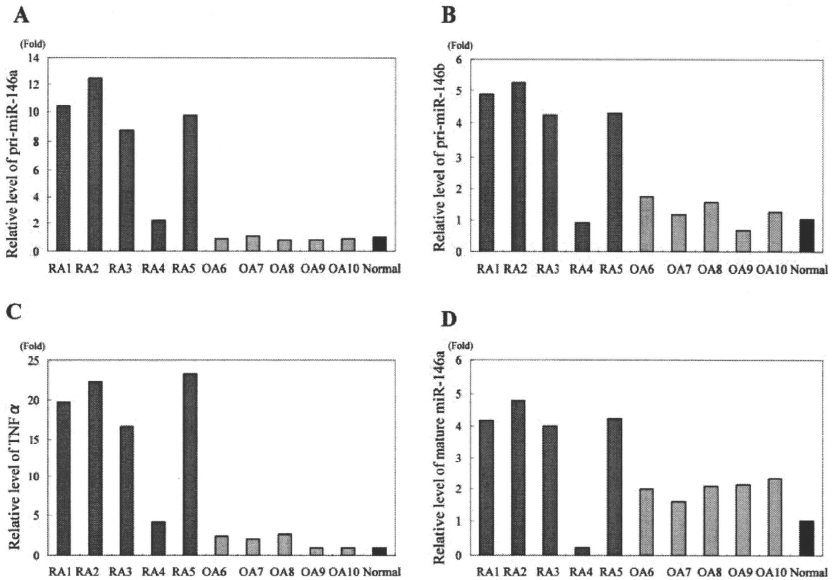

Figure 1. Quantitative reverse transcription–polymerase chain reaction analysis of the expression of primary microRNA-146a/b (pri-miR-146a/b), tumor necrosis factor α (TNFα), and mature miR-146a in synovial tissue from 5 patients with rheumatoid arthritis (RA), 5 patients with osteoarthritis (OA), and a normal control subject. GAPDH was used as an internal control for primary miR-146a/b and TNFα, and let-7a was used as an internal control for mature miR-146a. **A** and **B,** Primary miR-146a/b mRNA was strongly expressed in RA synovial tissue, except for that from patient RA4. In OA synovium, primary miR-146a/b expression was low. **C,** TNFα mRNA was expressed in the same pattern as that of primary miR-146a/b. Normal synovial tissue showed little primary miR-146a/b or TNFα mRNA expression. **D,** Mature miR-146a mRNA was more strongly expressed in synovial tissue from patients RA1, RA2, RA3, and RA5 than in tissue from patient RA4 and all of the OA patients.

Isogen reagent. Real-time PCR was performed in triplicate with the TaqMan microRNA assay kit to analyze the expression of mature miR-146a or with SYBR Green to analyze the expression of primary miR-146a/b. RT-PCR was conducted to analyze primary miR-146a/b and TNFα.

Statistical analysis. Data were analyzed statistically using the Mann-Whitney U test. *P* values less than 0.05 were considered statistically significant.

RESULTS

Expression of miR-146a/b and proinflammatory cytokine genes in synovial tissue. In the pathogenesis of RA, TNFα is an essential mediator of inflammation. To examine a potential link between miR-146a/b and RA inflammatory activity, mRNA for primary miR-146a/b and TNFα were analyzed by quantitative RT-PCR in normal synovial tissue and in synovial tissue from RA and OA patients (Figures 1A–C). Both primary miR-146a and miR-146b, and the mature form of miR-146a (Figure 1D) were strongly expressed in patients RA1, RA2, RA3, and RA5. TNFα expression (Figure 1C) was also up-regulated in synovial tissue from these patients. In synovial tissue from patient RA4, who had lower levels of RA activity compared with that in the other RA patients, neither the primary miR-146a/b nor TNFα mRNA was highly expressed.

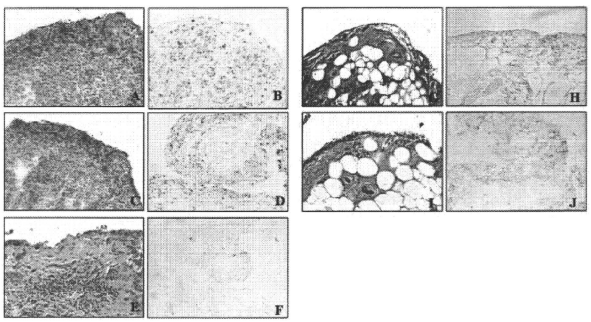

Figure 2. Hematoxylin and eosin (H&E) staining and in situ hybridization of synovial tissue from rheumatoid arthritis (RA) patients RA1 (**A** and **B**), RA3 (**C** and **D**), and RA4 (**E** and **F**) and from osteoarthritis (OA) patients OA7 (**G** and **H**) and OA8 (**I** and **J**). For each pair of images, H&E staining is shown on the left and in situ hybridization on the right. **A–D,** Synovial tissue from RA patients RA1 and RA3 show hyperplasia of the synovial tissue and infiltration of inflammatory cells, as demonstrated by H&E staining. In situ hybridization reveals primary microRNA-146a (miR-146a) expression in the superficial and sublining layers. **E** and **F,** Synovial tissue from patient RA4 shows fibrosis, but little infiltration of inflammatory cells, indicating remission of inflammation, as demonstrated by H&E staining. In situ hybridization reveals no expression of primary miR-146a. **G–J,** Synovial tissue from OA patients OA7 and OA8 consists mostly of adipose cells and shows little hyperplasia of the superficial and sublining layers, as demonstrated by H&E staining. In situ hybridization reveals little expression of primary miR-146a. (Original magnification × 200.)

In contrast, in OA synovium, expression of primary miR-146a/b and TNFα mRNA was low. Expression of primary miR-146a/b or TNFα was hardly detected in normal synovial tissue. These observations suggest that primary miR-146a/b expression may accompany synovial inflammation caused by TNFα.

We next examined the expression of mature miR-146a processed by Dicer using real-time PCR of synovial tissue specimens. Mature miR-146a was intensely expressed in patients RA1, RA2, RA3, and RA5 (Figure 1D). In these patients, the expression pattern of mature miR-146a was similar to that of primary miR-146b, suggesting that miR-146a/b up-regulation occurs at a transcription, rather than a maturation, step.

Expression of primary miR-146a in synovial tissue. To examine the expression of primary miR-146a in synovial tissue from RA and OA patients, we performed in situ hybridization. Primary miR-146a expression was seen in synovial tissue cells in the superficial and sublining layers of samples from all RA patients examined (Figure 2), except for patient RA4, in which the expression of miR-146 and proinflammatory cytokines as determined by RT-PCR was low (Figure 1). Hematoxylin and eosin staining of synovial tissue from patient RA4 revealed fibrosis and little infiltration of inflammatory cells in synovial tissue. Synovial tissue from the other RA patients showed vigorous proliferation of synovial cells and infiltration of inflammatory cells typical of the histopathologic changes of RA.

In synovial tissue from OA patients, hematoxylin and eosin staining revealed little hyperplasia and infiltration of inflammatory cells in the superficial and sublining layers. Superficial and sublining layers of the tissue from these patients showed little expression of primary miR-146a.

Identification of cells expressing miR-146 in RA synovial tissue. To identify the cells that expressed miR-146 in RA synovial tissue, we performed immunohistochemical analyses using the markers CD68 for macrophages, CD3ε for T cells, and CD79a for B cells, in combination with in situ hybridization (Figure 3). Expression of miR-146a mRNA was observed in cells distributed along the superficial and sublining layers. Double staining revealed that miR-146a+ cells were

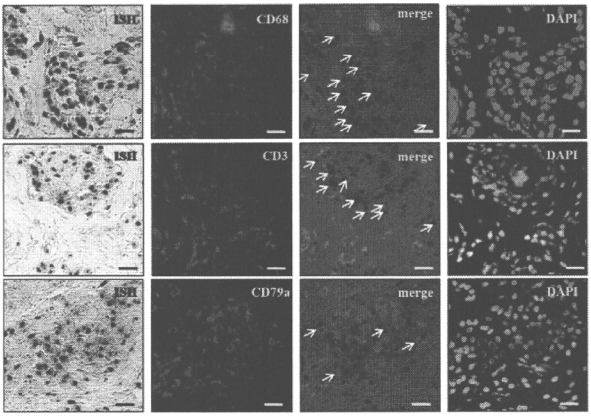

Figure 3. Double in situ hybridization and immunohistochemistry of rheumatoid arthritis (RA) synovial tissue. In situ hybridization (ISH) for primary microRNA146-a (miR-146a) and immunohistochemistry with CD68, CD3, and CD79a antibodies were performed on synovial tissue from patient RA5. Primary miR-146a was expressed in cells of the superficial and sublining layers, including mainly CD68+ macrophages, but some CD3+ T cells and CD79a+ B cells as well. **Arrows** in the merged images indicate cells expressing miR-146a and antibody markers. Staining of the tissue sections with 4′,6-diamidino-2-phenylindole (DAPI) is shown at the right. (Original magnification × 200; bars = 50 μm).

primarily CD68+, indicating that they were macrophages, but several CD3+ T cells and CD79a+ B cells were also seen.

Expression of miR-146 in RASFs induced by TNFα and IL-1β. We next evaluated the up-regulation of miR-146 expression in RASFs following stimulation with TNFα and IL-1β, as was previously described in THP-1 cells (20). Expression of mature miR-146a and primary miR-146a/b was significantly up-regulated in RASFs after TNFα and IL-1β stimulation (Figures 4A, C, and D). RT-PCR analysis showed that the expression of mRNA for primary miR-146a/b and TNFα was also induced after stimulation with these factors (Figure 4B).

DISCUSSION

Recently, a potential link between microRNA and several human diseases has been examined. For example, the expression of let-7 has been shown to be lower in lung cancer tissue than in normal lung tissue, and such down-regulation may promote high levels of expression of the Ras gene (23). It has also been shown that the expression of miR-143 and miR-145 is reduced in colon cancer tissue. Evidence of microRNA function in conditions such as leukemia, viral infection, and DiGeorge syndrome has been reported (24–29), and therapeutic trials aimed at silencing microRNA in vivo have been conducted (29,30).

The present study, which reveals that miR-146a/b is highly expressed in RA synovial tissue, is the first to focus on microRNA expression in the tissue from RA patients. Human miR-146a is located in the second exon of the LOC285628 gene on human chromosome 5, and human miR-146b resides on chromosome 10. Taganov et al (20) reported that miR-146a/b, miR-132, and miR-155 were identified among 200 microRNA after exposure of the human monocytic THP-1 cell line to LPS. Those authors focused particularly on miR-146a/b after validating levels of miR-146a/b, miR-132, and miR-155 by quantitative RT-PCR. In our analysis of RASFs, we observed strong induction of miR-146a following TNFα stimulation and did not observe up-regulation of miR-132 or miR-155 (data not shown).

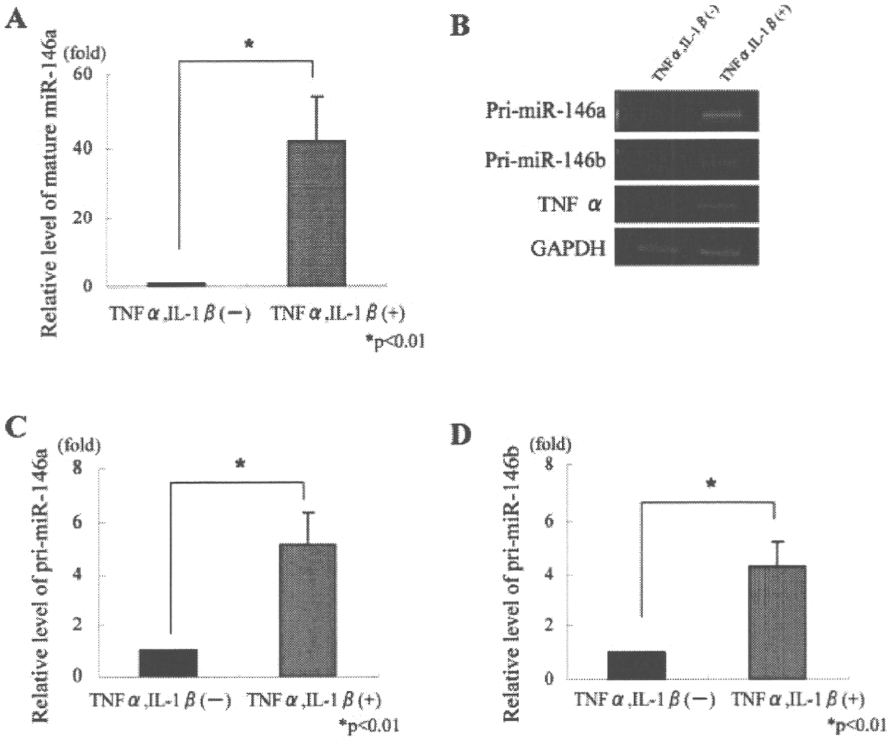

Figure 4. Induction of primary microRNA-146a/b (pri-miRNA-146a/b) and mature miR-146a microRNA expression in rheumatoid arthritis synovial fibroblasts (RASFs) stimulated with tumor necrosis factor α (TNFα) and interleukin-1β (IL-1β). **A,** Expression of mature miR-146a, as determined by reverse transcription–polymerase chain reaction (RT-PCR) analysis. Mature miR-146 expression in RASFs was significantly increased after TNFα and IL-1β stimulation. **B,** Expression of mRNA for primary miR-146a (pri-miR-146a), primary miR-146b, and TNFα by RT-PCR analysis, normalized to GAPDH expression. Primary miR-146a/b and TNFα mRNA expression in RASFs increased following TNFα and IL-1β stimulation. **C** and **D,** Expression of primary miR-146a (**C**) and primary miR-146b (**D**), as determined by quantitative RT-PCR analysis. Primary miR-146a/b expression was significantly up-regulated by TNFα and IL-1β stimulation. Bars show the mean and SD of triplicate experiments. *P* values were determined by Mann-Whitney U test.

The results of our in situ hybridization and immunohistochemical analyses indicated that miR-146a is expressed in various cell types in the superficial and sublining layers of synovial tissue, including synovial fibroblasts, macrophages, T cells, and B cells. In RA, activated CD4+ T cells stimulate macrophages and synovial fibroblasts. These cells secrete inflammatory cytokines, such as TNFα and IL-1β, which also contribute to the formation of hyperplastic synovium, called pannus. It is possible that miR-146a/b might play a role in these pathologic conditions. Moreover, our results also show that miR-146a/b expression could be induced by stimulation with TNFα and IL-1β, which implies that miR-146 mRNA are expressed in synovial fibroblasts in response to TNFα and IL-1β. In our small series of patients, all of the RA patients were being treated with corticosteroids, and 2 patients were also receiving a DMARD. Thus, the influence of drug therapy on miR-146 expression could not be evaluated in our study. Whether or how drug therapy influences miR-146 expression should be clarified in future studies.

Taganov et al (20) reported that miR-146a/b targets are TRAF6 and IRAK1, which are key molecules downstream of TNFα and IL-1β signaling. Those authors concluded that miR-146a/b might play a pivotal role in the fine regulation of a Toll-like receptor and cytokine signaling through negative feedback involving the down-regulation of TRAF6 and IRAK1. If similar

processes occur in the pathogenesis of RA, miR-146a/b may function in the termination of inflammation triggered by TNFα and IL-1β. On the other hand, Monticelli et al (31), using microarray and Northern blot analysis in a murine hematopoietic system, demonstrated that miR-146 expression is higher in Th1 cells than in Th2 or naive T cells. Several other studies have shown that Th1 cells dominate in the balance of Th1/Th2 cells in RA (32,33). Gerli et al (34) noted that Th1 cells drive the condition in RA and that Th2 cells respond early in the disease process. A subset of Th1 cells that produces IL-2, IL-12, and IFNγ may activate macrophages in RA (35). Relevant to this, our data indicate that accumulated CD3+ cells express miR-146, which suggests that miR-146 might play a role in persistent inflammation in RA via a T cell network. Further functional analyses to determine the precise role of miR-146a/b in the pathogenesis of RA could provide novel diagnostic and/or therapeutic tools.

AUTHOR CONTRIBUTIONS

Dr. Asahara had full access to all of the data in the study and takes responsibility for the integrity of the data and the accuracy of the data analysis.

Study design. Nakasa, Miyaki, Asahara.

Acquisition of data. Nakasa, Miyaki, Okubo, Nishida, Ochi,

Analysis and interpretation of data. Miyaki, Okubo, Hashimoto, Nishida, Asahara.

Manuscript preparation. Nakasa, Asahara.

Statistical analysis. Nakasa, Hashimoto.

REFERENCES

1. Gardner DL. Rheumatoid arthritis: cell and tissue pathology. In: Pathological basis of the connective tissue diseases. London: Edward Arnold; 1992. p. 444–526.
2. Lipsky PE, van der Heijde DM, St.Clair EW, Furst DE, Breedveld FC, Kalden JR, et al, for the Anti–Tumor Necrosis Factor Trial in Rheumatoid Arthritis with Concomitant Therapy Study Group. Infliximab and methotrexate in the treatment of rheumatoid arthritis. N Engl J Med 2000;343:1594–602.
3. Bresnihan B, Alvaro-Gracia JM, Cobby M, Doherty M, Domljan Z, Emery P, et al. Treatment of rheumatoid arthritis with recombinant human interleukin-1 receptor antagonist. Arthritis Rheum 1998;41:2196–204.
4. Barnes PJ, Karin M. Nuclear factor-κB: a pivotal transcription factor in chronic inflammatory diseases. N Engl J Med 1997;336: 1066–71.
5. Tak PP, Firestein GS. NF-κB: a key role in inflammatory diseases. J Clin Invest 2001;107:7–11.
6. Handel ML, McMorrow LB, Gravallese EM. Nuclear factor-κB in rheumatoid synovium: localization of p50 and p65. Arthritis Rheum 1995;38:1762–70.
7. Asahara H, Asanuma M, Ogawa N, Nishibayashi S, Inoue H. High DNA-binding activity of transcription factor NF-κB in synovial membranes of patients with rheumatoid arthritis. Biochem Mol Biol Int 1995;37:827–32.
8. Marok R, Winyard PG, Coumbe A, Kus ML, Graffney K, Blades S, et al. Activation of the transcription factor nuclear factor-κB in human inflamed synovial tissue. Arthritis Rheum 1996;39:583–91.
9. Romanshkova JA, Makarov SS. NF-κB is a target of AKT in apoptotic PDGF signaling. Nature 1999;401:86–90.
10. Guttridge DC, Albanese C, Reuther JY, Pestell RG, Baldwin AS Jr. NF-κB controls cell growth and differentiation through transcriptional regulation of cyclin D1. Mol Cell Biol 1999;19:5785–99.
11. Ambros V. The functions of animal microRNAs. Nature 2004;431: 350–5.
12. Bartel DP. MicroRNAs: genomics, biogenesis, mechanism, and function. Cell 2004;116:281–97.
13. Farh KK, Grimson A, Jan C, Lewis BP, Johnson WK, Lim LP, et al. The widespread impact of mammalian microRNAs on mRNA repression and evolution. Science 2005;310:1817–21.
14. Denli AM, Tops BB, Plasterk RH, Ketting RF, Hannon GJ. Processing of primary microRNAs by the Microprocessor complex. Nature 2004;432:231–5.
15. Gregory RI, Yan KP, Amuthan G, Chendrimada T, Doratotaj B, Cooch N, et al. The Microprocessor complex mediates the genesis of microRNAs. Nature 2004;432:235–40.
16. Lee Y, Ahn C, Han J, Choi H, Kim J, Yim J, et al. The nuclear RNase III Drosha initiates microRNA processing. Nature 2003; 425:415–9.
17. Chendrimada TP, Gregory RI, Kumaraswamy E, Norman J, Cooch N, Nishikura K, et al. TRBP recruits the Dicer complex to Ago2 for microRNA processing and gene silencing. Nature 2005; 436:740–4.
18. Calin GA, Sevignani C, Dumitru CD, Hyslop T, Noch E, Yendamuri S, et al. Human microRNA genes are frequently located at fragile sites and genomic regions involved in cancers. Proc Natl Acad Sci U S A 2004;101:2999–3004.
19. Lecellier CH, Dunoyer P, Arar K, Lehmann-Che J, Eyquem S, Himber C, et al. A cellular microRNA mediates antiviral defense in human cells. Science 2005;308:557–60.
20. Taganov KD, Boldin MP, Chang KJ, Baltimore D. NF-κB-dependent induction of microRNA miR-146, an inhibitor targeted to signaling proteins of innate immune responses. Proc Natl Acad Sci U S A 2006;103:12481–6.
21. Arnett FC, Edworthy SM, Bloch DA, McShane DJ, Fries JF, Cooper NS, et al. The American Rheumatism Association 1987 revised criteria for the classification of rheumatoid arthritis. Arthritis Rheum 1988;31:315–24.
22. Nishida K, Komiyama T, Miyazawa S, Shen ZN, Furumatsu T, Doi H, et al. Histone deacetylase inhibitor suppression of autoantibody-mediated arthritis in mice via regulation of $p16^{INK4a}$ and $p21^{WAF1/Cip1}$ expression. Arthritis Rheum 2004;50:3365–76.
23. Johnson SM, Grosshans H, Shingara J, Byrom M, Jarvis R, Cheng A, et al. RAS is regulated by the let-7 microRNA family. Cell 2005;120:635–47.
24. Michael MZ, O'Conner SM, van Holst Pellekaan NG, Young GP, James RJ. Reduced accumulation of specific microRNAs in colorectal neoplasia. Mol Cancer Res 2003;1:882–91.
25. Calin GA, Dumitru CD, Shimizu M, Bichi R, Zupo S, Noch E, et al. Frequent deletions and down-regulation of micro-RNA genes miR15 and miR16 at 13q14 in chronic lymphocytic leukemia. Proc Natl Acad Sci U S A 2002;99:15524–9.
26. Calin GA, Ferracin M, Cimmino A, Di Leva G, Shimizu M, Wojcik SE, et al. A microRNA signature associated with prognosis and progression in chronic lymphocytic leukemia [published erratum appears in N Engl J Med 2006;355:533]. N Engl J Med 2005;353:1793–801.
27. Pfeffer S, Zavolan M, Grasser FA, Chien M, Russo JJ, Ju J, et al. Identification of virus-encoded microRNAs. Science 2003;304: 734–6.
28. Landthaler M, Yalcin A, Tuschl T. The human DiGeorge syn-

drome critical region gene 8 and its D. melanogaster homolog are required for miRNA biogenesis. Curr Biol 2004;14:2162–7.
29. Krutzfeldt J, Rajewsky N, Braich R, Rajeev KG, Tuschl T, Manoharan M, et al. Silencing of microRNAs in vivo with 'antagomirs.' Nature 2005;438:685–9.
30. Yang B, Lin H, Xiao J, Lu Y, Luo X, Li B, et al. The muscle-specific microRNA miR-1 regulates cardiac arrhythmogenic potential by targeting GJA1 and KCNJ2. Nat Med 2007;13:486–91.
31. Monticelli S, Ansel KM, Xiao C, Socci ND, Krichevsky AM, Thai TH, et al. MicroRNA profiling of the murine hematopoietic system. Genome Biol 2005;6:R71.
32. Shulze-Koops H, Kalden JR. The balance of Th1/Th2 cytokines in rheumatoid arthritis. Best Pract Res Clin Rheumatol 2001;15: 677–91.
33. Da Silva JA, Spector TD. The role of pregnancy in the course and aetiology of rheumatoid arthritis. Clin Rheumatol 1992;11:189–94.
34. Gerli R, Bistoni O, Russano A, Fiorucci S, Borgato L, Cesarotti ME, et al. In vivo activated T cells in rheumatoid synovitis: analysis of Th1- and Th2-type cytokine production at clonal level in different stages of disease. Clin Exp Immunol 2002;129:549–55.
35. Murphy KM, Reiner SL. The lineage decisions of helper T cells. Nat Rev Immunol 2002;2:933–44.